Foundations of Physics, Vol. 22, No. 10, 1992

Wave–Particle Dualism and the Interpretation of Quantum Mechanics

C. Dewdney,[1] G. Horton,[1] M. M. Lam,[1] Z. Malik,[1] and M. Schmidt[2]

Received July 7, 1992

The realist interpretations of quantum theory, proposed by de Broglie and by Bohm, are re-examined and their differences, especially concerning many-particle systems and the relativistic regime, are explored. The impact of the recently proposed experiments of Vigier et al. and of Ghose et al. on the debate about the interpretation of quantum mechanics is discussed. An indication of how de Broglie and Bohm would account for these experimental results is given.

Contents

1. Introduction 1218
2. Realist Interpretations of Quantum Theory 1219
   2.1. Bohm's Causal Interpretation 1219
   2.2. de Broglie's Theory of the Double Solution 1220
   2.3. The Pilot-Wave Theory 1221
3. Bohr's Interpretation of Quantum Mechanics 1222
4. Tunneling and Quantum Interference 1224
   4.1. Tunneling 1224
   4.2 Neutron Interferometry 1227
5. Differences between de Broglie and Bohm in the Nonrelativistic, Many-Body Case 1230
   5.1. Quantum Statistics: Two Particles in a Harmonic-Oscillator Potential 1230
   5.2. Waves in Real Space? 1236
6. Relativistic Fermion Systems 1237
   6.1. Dirac Trajectories 1238
      6.1.1. Plane-Wave Solutions 1239
      6.1.2. Superposition of Plane Waves 1240

[1] Department of Applied Physics, University of Portsmouth, Portsmouth PO1 2DZ, United Kingdom.
[2] Department of Physics, University of Bremen, Bremen, Germany.

0015-9018/92/1000-1217$06.50/0

7. Bohm's Quantum Field Theory for Bosons 1243
7.1. Anticorrelation between Two Atoms in a One-Photon Field . . 1246
8. Relativistic Boson Particle Trajectories? 1256
9. Experimental Distinctions between the Different Interpretations of Quantum Mechanics? 1259
9.1. The Detection of the Broglie Waves 1260
9.2. The Experiment of Vigier *et al.* 1261
9.3. The Experiment of Ghose *et al.* 1263
10. References 1264

1. INTRODUCTION

Given the volume of material that has been published on the subject of the interpretation of quantum theory, it is clearly not an exaggeration to claim that the fundamental issues remain unresolved. Many approaches to the interpretation of quantum mechanics and their ramifications have been discussed at length, but a survey of the literature reveals that the amount of debate devoted to those realist interpretations proposed by de Broglie[1,2] and by Bohm[3] is very small. Where these latter approaches are considered they are often quickly rejected, either through misunderstanding or as a matter of taste. Furthermore, the different approaches to the interpretation of quantum theory proposed by de Broglie and by Bohm are frequently conflated, and it is part of our purpose here to reiterate the essential differences between them. The points of distinction are most evident in the description of many-body systems, in the nonrelativistic domain, and in the description of relativistic bosons.

We shall first review, in Section 2, the formalism of Bohm's causal interpretation and of de Broglie's double solution. This shall be done in the nonrelativistic single-particle case since many of the fundamental problems of interpretation can be formulated in this simple context. In Sec. 3 we question the validity of the assumptions made by Bohr in formulating his interpretation of quantum mechanics and also the resulting limitations on our ability to describe quantum systems. In Sec. 4 we present a causal account of quantum interference and tunneling and then proceed to illustrate, in Sec. 5, the differences between the approaches of Bohm and de Broglie, using a system consisting of two particles in a harmonic-oscillator potential.

The principles of the extension of these models to relativistic many-fermion systems will then be presented in Sec. 6. Following this discussion we examine, in Sec. 7, the approach to boson fields suggested by Bohm, applying it to a simple model of two atoms interacting with a single-mode scalar cavity field. The purpose of doing this is to bring out clearly the

way in which Bohm's quantum field theory accounts for the anticorrelation in the firing of two detectors interacting with a single photon field. We then proceed to discuss, in Sec. 8, the radically different approaches to relativistic boson systems proposed by Bohm and by de Broglie, including the problems involved in defining trajectories for relativistic bosons.

Recently Vigier *et al.*[4] and Ghose *et al.*[5] have each proposed experiments which they claim can elucidate the problem of the interpretation of quantum mechanics. The experiment proposed by the former group concerns neutron interferometry and that of the latter group concerns a single-photon anticorrelation experiment. In the last section we use these experiments as a basis for deliberation concerning matters of interpretation, making use of the foregoing descriptions of related, but simplified, model systems presented in Secs. 4 and 7.1. In particular, we compare the details of the trajectory interpretations of Bohm and de Broglie with the interpretation proposed by Bohr.

2. REALIST INTERPRETATIONS OF QUANTUM THEORY

2.1. Bohm's Causal Interpretation

Formally, Bohm's causal interpretation of quantum mechanics arises when the substitution

$$\psi = R\, e^{iS/\hbar} \tag{1}$$

is made in the Schrödinger equation

$$\left(-\frac{\hbar^2}{2m}\nabla^2 + V\right)\psi = i\hbar\frac{\partial\psi}{\partial t} \tag{2}$$

and the real and imaginary parts are separated, yielding the equations

$$\frac{\partial\rho}{\partial t} + \nabla\cdot(\rho\mathbf{v}) = 0 \tag{3}$$

and

$$-\frac{\partial S}{\partial t} = -\frac{\hbar^2}{2m}\frac{\nabla^2 R}{R} + \frac{(\nabla S)^2}{2m} + V \tag{4}$$

where $\rho = |\psi|^2$ and

$$m\mathbf{v} = \nabla S \tag{5}$$

Equation (3) expresses the conservation of probability density; this is interpreted as the probability density for the particle to *be* at a certain position. This probability is not inherent in the conceptual structure of the theory, but is a consequence of the necessary lack of knowledge of the precise initial particle coordinates. Equation (4) can be interpreted as a Hamilton–Jacobi equation, with an extra "quantum potential" term, Q, given by

$$Q = -\frac{\hbar^2}{2m}\frac{\nabla^2 R}{R} \tag{6}$$

We also have an expression for the "quantum force" due to the quantum potential:

$$\mathbf{F} = -\nabla(Q + V) = -\nabla V_{\text{eff}} \tag{7}$$

In this approach to quantum mechanics, the real existents are the ψ-field and the actual particle position. A given initial ψ-field, initial particle position, and Hamiltonian yield a unique individual evolution for the particle. The trajectories are the integral curves of (5)[3] and since S is determined by (2), the trajectory of an individual particle and the evolution of its dynamical variables are determined by the development of ψ. A single quantum-mechanical object consists of both a particle and an objectively real wave which guides the particle. All of the predictions of quantum mechanics can be accounted for in terms of a well-defined conceptual scheme, and many detailed calculations have now been carried out demonstrating exactly how the Bohm approach works in specific cases in the nonrelativistic regime.

2.2. de Broglie's Theory of the Double Solution

Ideas similar to those of Bohm were first investigated by de Broglie in the 1920's.[2] According to de Broglie's "principle of the double solution," every continuous solution of the Schrödinger equation, (2), has a corresponding singularity solution

$$u(x, y, z, t) = f(x, y, z, t)\, e^{iS(x, y, z, t)/\hbar} \tag{8}$$

which shares the same phase as ψ, but has an amplitude, $f(x, y, z, t)$, involving a mobile singular region. The amplitude of $u(x, y, z, t)$ is exactly

[3] John Bell, who was very sympathetic to trajectory interpretations, believed that the only equation necessary to these interpretations is (5). He felt that the full Hamilton–Jacobi theory was an unnecessary complication.

the same as the one for ψ except within a spherical singular region, O. The theoretical ideas behind Bohm's quantum potential approach and the Broglie's theory of the double solution are quite different and, unlike Bohm, de Broglie only successfully completed his theory in the single particle case.

In the theory of the double solution for a single particle, the quantum object consists of a physical wave in real space, given by $u(x, y, z, t)$. It is the presence of the singularity in u which gives rise to the particle-like behavior. So, unlike Bohm, de Broglie does not have to postulate the existence of the particle; he provides a more natural explanation of the dependence of the movement of the particle on the development of the wave. According to de Broglie, the wavefunction of quantum mechanics is considered to be of statistical signification and not real since, in the many particle case, the wavefunction necessarily exists in configuration space. He considered the u-waves, in real space, to represent reality and his aim (which he never achieved) was to reproduce many-particle quantum mechanics using these u-waves.

2.3. The Pilot-Wave Theory

In 1927 de Broglie presented his ideas on the theory of the double solution in a simpler form, under the title of "the pilot-wave theory." For the case of a single particle, the pilot-wave theory is identical in form to the theory of Bohm—the wavefunction guides the movement of the particle, accounting for the wave-particle duality observed in quantum mechanical systems. We obtain the pilot-wave theory from the theory of the double solution in the following way: if the single particle solution for u is used in the Schrödinger equation, for the region outside O, we obtain similar equations to those found by Bohm, i.e., (3) and (4), except that now the amplitude $R(x, y, z, t)$ is replaced by the amplitude $f(x, y, z, t)$. de Broglie's version of the continuity equation is

$$\frac{\partial f}{\partial t} = -\frac{1}{2m}(f\nabla^2 S + 2\nabla f \nabla S) \tag{9}$$

de Broglie assumed that the function $S(x, y, z, t)$ holds the same value everywhere on the sphere O, as do its first derivatives. The function $f(x, y, z, t)$, however, does not have the same value on all points of Q and increases very rapidly inside O. This means that if r is the route followed by the singularity, then $\partial f/\partial r$ is greater in magnitude than f (on the surface O) and the ratio $f/(\partial f/\partial r)$ is approximately zero. Dividing (9) by $-\partial f/\partial r$

and taking $f/(\partial f/\partial r) = 0$, we obtain the displacement velocity v_r of the value of the amplitude $f(x, y, z, t)$ on a point on the sphere O,

$$v_r = \frac{\nabla S}{m} \tag{10}$$

This equation for the velocity of the singularity is known as the "guidance formula." It shows that the velocity is derived from the phase $S(x, y, z, t)$, which is the same for both the wavefunction ψ and the u-wave solution (8). The simpler pilot-wave theory is able to avoid any reference to the u-wave and just assumes instead that a single particle is guided in its motion by the wavefunction, according to the guidance formula, as in Bohm's theory.

3. BOHR'S INTERPRETATION OF QUANTUM MECHANICS

In this section we discuss how the Copenhagen interpretation accounts for the observed behavior of quantum mechanical systems such as the experiment of Vigier *et al.*, described in Sec. 9.2. In particular, we will demonstrate that not only are we free to choose a deterministic description for a quantum mechanical system of particles, in terms of particle trajectories, but that such an interpretation of the theory provides a far more powerful analysis of quantum mechanical systems than is provided by the orthodox interpretation.

The Copenhagen interpretation is considered by many physicists to be the usual interpretation of quantum mechanics. A fact which has often been overlooked with regard to this interpretation is that we are not forced by experimental evidence to adopt it; there is no need to restrict the description of physics to that of classical physics or to relinquish a causal description of the quantum domain, as is claimed by this interpretation, and we suggest that any interpretation which does not have to do either of these two things has an advantage over the Copenhagen interpretation.

The Copenhagen interpretation is difficult to present in a clear and unambiguous form. This is partly because it consists of many differing viewpoints, the most influential being that of Bohr, but with important and quite distinct ideas being contributed from, among others, von Neumann, Heisenberg, Born and Pauli; however, if we confine ourselves for the moment to the interpretation of Bohr,[6,7] it is also apparent that his ideas alone, although self-consistent, are vague and assume an unnecessary degree of restriction on the possible forms of description of quantum phenomena.

Bohr proposed that (i) all unambiguous descriptions of physical systems must be made using the terminology of classical physics and that

(ii) a direct description of quantum mechanical systems is beyond the abilities of the classical framework. He restricted the role of physics to making statements exclusively about the instruments which are used in the preparation and observation of quantum systems, since he assumed that these could be correctly described by classical physics.

Because Bohr assumed that a description of a quantum system was not possible without the classical measuring apparatus, he considered it impossible to draw any conclusions about the properties of the quantum system alone or to ascribe individual properties to the system, independently of the experimental arrangement. Thus a suitably chosen measuring apparatus is able to provide a single, stable result for the measurement of a specific physical quantity (and for variables which commute with this quantity), but, in general, it cannot provide a measurement of all quantities. For instance, it is not possible to make a measurement of both particle position and momentum simultaneously, within one experimental set-up. According to Bohr's interpretation, reference to a physical quantity is only meaningful in the context of an appropriate measurement of that quantity, and any reference to a quantity which cannot be measured is meaningless.

This means that the concept of a particle trajectory (and indeed any causal and continuous description of a quantum system) is meaningless, since no apparatus is suitable for making a measurement of both the position and momentum of a quantum particle. Bohr termed pairs of variables which do not commute, such as position and momentum, "complementary pairs." He asserted that the wave and particle aspects of quantum objects from such a complementary pair, resulting in the impossibility of describing the behavior of quantum systems using the concepts of "wave" and "particle" simultaneously. If we consider the experiment of Vigier *et al.*, described in Sec. 9.2, which concerns the wave–particle duality of neutrons in an interferometer, this interpretation is unable to account for the interference of single neutrons in terms of trajectories. It is meaningless to refer to the motion of the neutron-particle in space and time through the apparatus, the complete description of the experiment being contained in the wavefunction which provides solely a statistical account of measurements.

The aim of Bohr's interpretation was to provide a consistent and unambiguous way of describing our interaction with quantum systems; however, without even demonstrating that it is necessary, Bohr has imposed on quantum mechanics the necessity of using classical terminology, and in doing so has relinquished a description in terms of cause and effect. The lack of, firstly, a causal description of quantum events and, secondly, a formal theory for the measurement process, considered by Bohr

to be so crucial, results in an interpretation which is difficult to understand and which fails to provide us with any picture of the quantum world at all. In the words of John Bell,[8] "vagueness, subjectivity, and indeterminism are not forced on us by experimental facts but by deliberate theoretical choice."

4. TUNNELING AND QUANTUM INTERFERENCE

In this section we discuss some illustrative examples of one-particle quantum effects. In the following, we only refer to the theory of Bohm but, as we have seen, in the single-particle case Bohm's theory coincides with the pilot-wave form of the theory of de Broglie.

In studying Bohm's theory it is important to scrutinise explicit calculations, in order to understand the subtle manner in which the usual results of quantum mechanics are recovered. For the purposes of this paper, we choose to discuss quantum interference and quantum tunneling, because of their relevance to the experiments of Vigier *et al.* and Ghose *et al.*, which we examine later, in Secs. 9.2 and 9.3. One practical difficulty with the approaches of de Broglie and Bohm is that there are very few cases in which particle trajectories can be calculated analytically, even when the velocity field is known in closed form. Furthermore, in many cases it is necessary to resort to numerical integration of the Schrödinger equation in order to calculate the evolution of the wavefunction on which the trajectories depend.

4.1. Tunneling

In order to see how the Bohm theory accounts for the phenomenon of quantum tunneling, detailed calculations have been carried out[9] for the scattering of a Gaussian wavepacket from various potentials.[4] Here we present the results for the scattering of a Gaussian wavepacket from a square potential barrier when the incident energy is less than the barrier height; the parameters of the scattering have been chosen to yield a transmission ratio of 0.5. Figure 1 shows a set of frames from a computer-generated motion picture of this process, and Fig. 2 shows a corresponding set of trajectories (x versus t). Note how the quantum potential modifies the classical square potential and allows those particles in the forward part of the wave packet to enter and pass through the classically forbidden region. One can see in this simple example that once the particle position and the wavefunction (the "hidden" parameters) are specified, along with

[4] A computer program and a video tape are available from C. Dewdney.

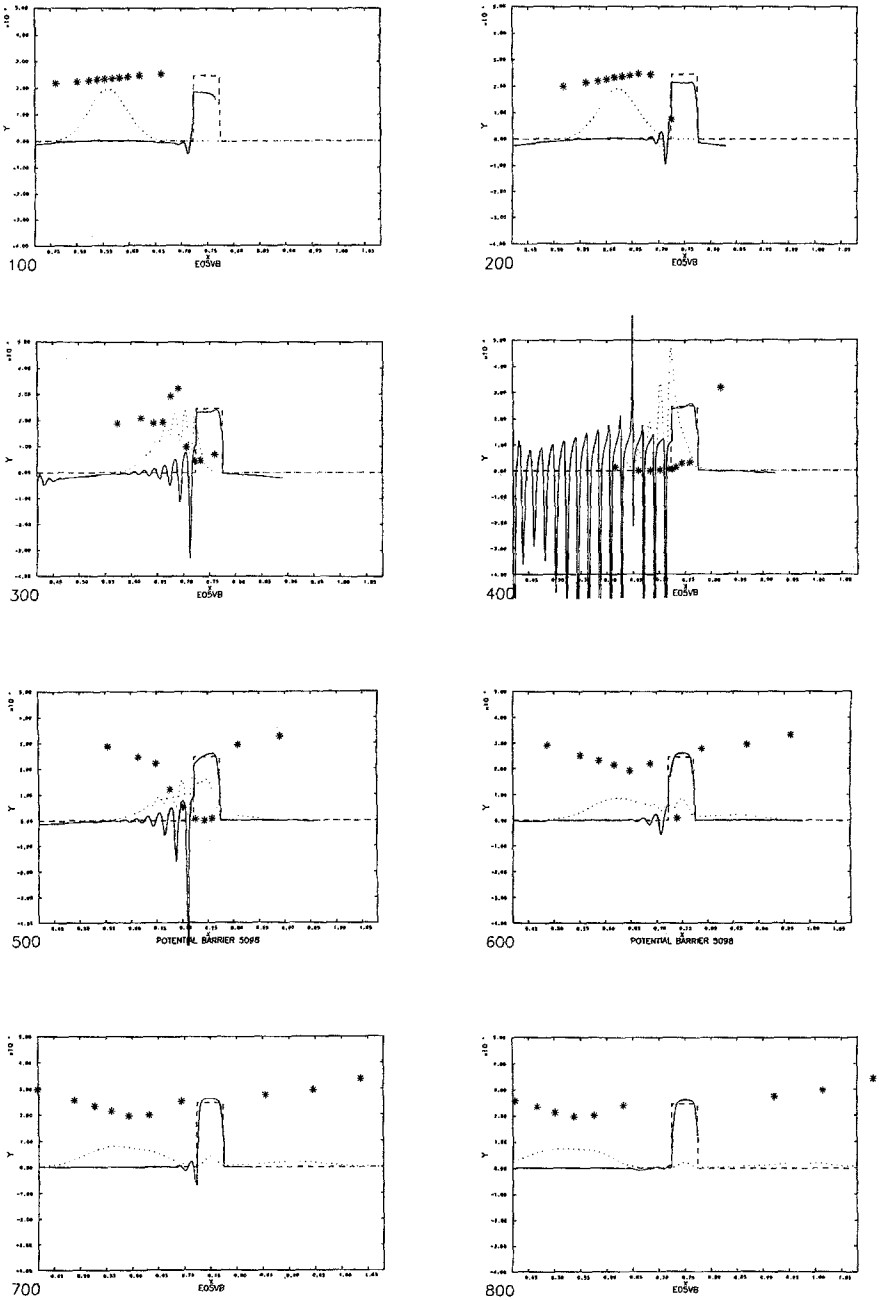

Fig. 1. A series of frames taken from a computer-generated motion picture, illustrating how tunneling occurs ion Bohm's theory. The dashed line represents the classical square potential, the solid line represents the effective potential, the dotted line represents the probability density, and the asterisks represent a set of possible particle motions (their order is maintained and the height in the frame represents the particle's energy).

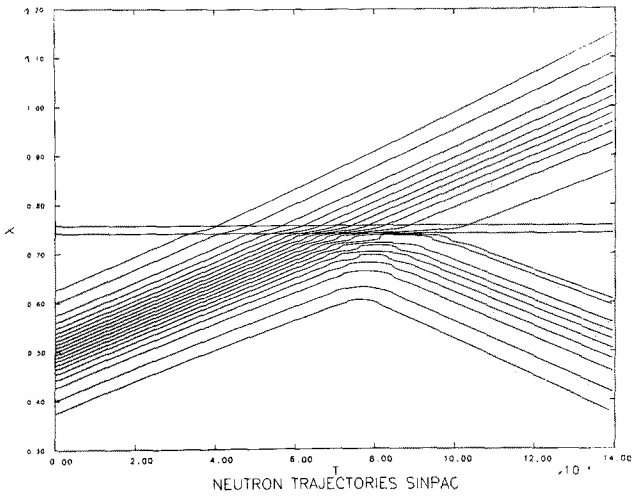

Fig. 2. A set of possible particle trajectories for a Gaussian wave packet incident on a square potential barrier (represented by the parallel lines).

the potential, the scattering process is described in a completely deterministic way. Whether, in an individual case, a particular particle is reflected from or transmitted through this potential (with acts as a beam splitter) is determined by its initial position in the wavepacket. The anticorrelation of the responses of two detectors, one placed in the path of the transmitted beam and the other in the reflected beam, has a simple explanation; in each case, the particle is actually either passed through the barrier or reflected from it, and so it interacts with just one detector.

After scattering, the wavefunction is a superposition of two separating packet states, with two corresponding sets of trajectories. However, the fact that the wavefunction is in a superposition of position states does not imply, in the Bohm theory, that the position is not definite. Neither does a definite position deny the possibility of subsequent interference. Both the wave and the particle aspects of matter have objective significance. If two spatially separated components of the wavefunction subsequently have cause to overlap, and if no interactions have taken place, then an interference pattern is created and the particle trajectories evolve in a manner consistent with this pattern. However, if the transmitted beam (for example) interacts with some device capable of recording the passage of the particle before the components overlap, then no interference will ensue on recombination of the beams. This is accounted for by the fact that the wavefunction of the particle–apparatus combination consists, after

measurement, of two orthogonal components. In this case the interference terms will vanish due to the orthogonality of the detector states "fired" and "not fired."

In the Bohm theory, the problem of accounting for the fact that individual events occur in individual experiments, even when the final wavefunction is a superposition, is solved by the trivial assumption of the existence of a definite trajectory for all the dynamical coordinates of the system. Thus, in an individual scattering of one particle from the square potential, the detector in the transmitted beam will either be excited or remain in its ground state, depending simply on the initial coordinate of the particle. Of course, the system may be extended to include observers, their friends and so on; but each part will in fact have a definite set of coordinates correlated with the actual particle coordinate.

Two points should be stressed here; firstly the statistical predictions of quantum theory are recovered if the initial distribution of the particles in an ensemble of experiments is given by $|\Psi|^2$.[5] Secondly, it is not possible to control the initial position of the particle in the wavepacket so that, in practice, the scattering of a particle from a beam splitter cannot be controlled, giving the appearance of randomness.

4.2. Neutron Interferometry

A simple one-dimensional model of an interferometer can be constructed by arranging for the reflected and transmitted wavepackets from the beam splitter, discussed in Sec. 4, to be reflected back onto the same beam splitter, subjecting one of the packets to a phase-shift before recombination. This is a valid procedure since, referring to Fig. 3, one sees that the significant component of the motion is perpendicular to the beam splitters.

[5] Arguments have been given which show that any distribution other than $|\Psi|^2$ will decay into a $|\Psi|^2$ distribution given certain reasonable assumptions which we shall not enter into here but are contained in Ref. 48.

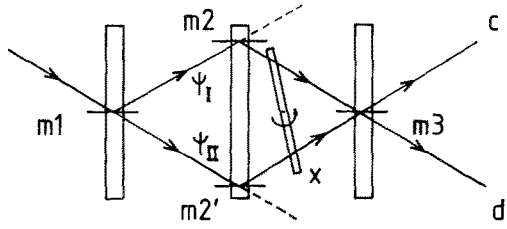

Fig. 3. A diagram of the neutron interferometry apparatus.

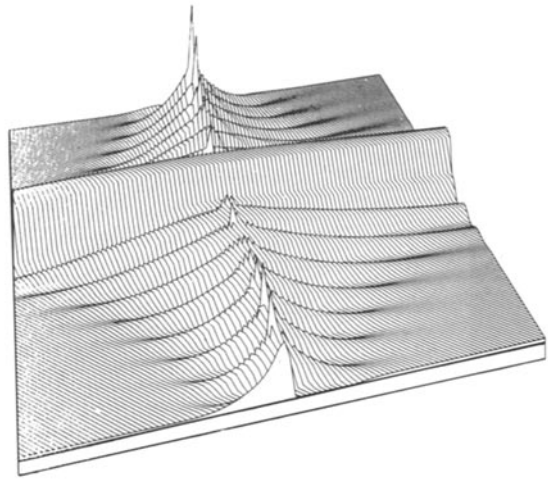

Fig. 4. The effective potential (quantum potential plus square barrier potentail), at the last beam splitter (M3), in the model of the neutron interferometer. The phase shift between the beams is $\pi/2$.

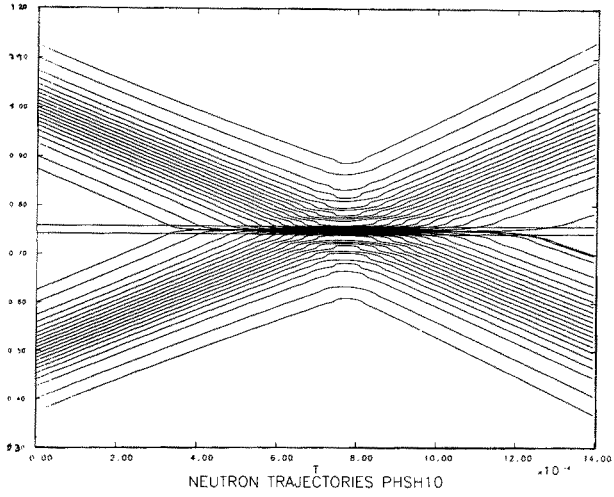

Fig. 5. The trajectories produced when two beams, which have passed through the interferometer, are recombined at the last beam splitter (M3). There is a phase shift of $\pi/2$ between the beams.

Detailed calculations have been carried out, using the Bohm theory, for both spatial and spin interference. The spatial interference observed in a neutron interferometer has been calculated and discussed in Ref. 10 while spin superposition has been discussed in Refs. 11 and 12. The motion of an individual neutron in a spin-flip coil has also been calculated, using the nonrelativistic approach to spin developed by Bohm, Schiller, and Tiomno[13]; the results are discussed by two of us in (C.D. and M.M.L.).[14] However, since in the experiment of Vigier *et al.* discussed later, both neutron beams have their spin inverted before recombination, the spin plays no role in the interference process at the final set of crystal planes, and we do not enter into a discussion of this part of the process.

We show the effective potential (classical potential plus quantum potential) and the associated trajectories for the recombination of the beams at the last beam splitter in Figs. 4–7. Figures 4 and 5 are calculated for the case in which the phase shift is such that the two emerging beams have equal amplitude (i.e., a phase-shift of $\pi/2$). One sees that the effective potential is such that no trajectories cross the line of symmetry. This could be deduced without explicit calculation; since the phase must be single-valued, the trajectories may not cross. Clearly, there is no conflict between particle paths through the interferometer and the occurrence of interference in the Bohm approach; the quantum potential is derived from the wave-function which contains information about the conditions present in both paths of the interferometer. This means, of course, that a phase shift

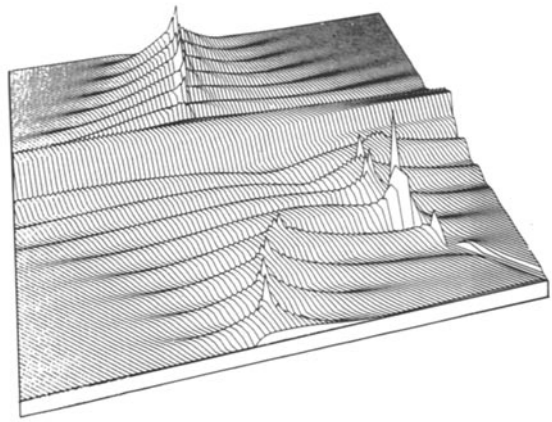

Fig. 6. The effective potential (quantum potential plus square barrier potential), at the last beam splitter (M3), in the model of the neutron interferometer. The phase shift between the beams is π.

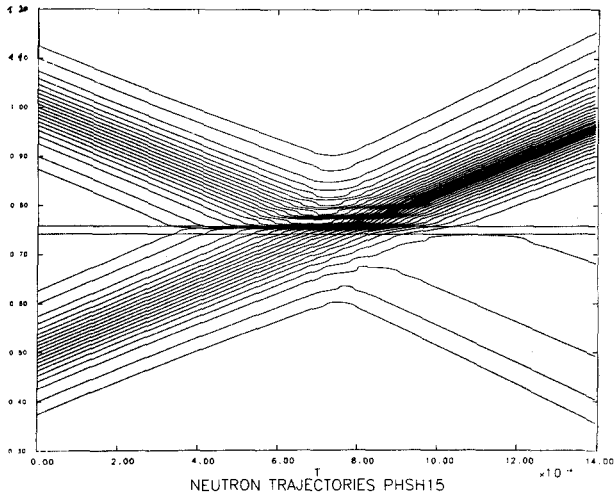

Fig. 7. The trajectories produced when two beams, which have passed through the interferometer, are recombined at the last beam splitter (M3). There is a phase shift of $\pi/2$ between the beams.

applied on one path will nevertheless affect the motion of the neutron in the interference region, even if it passed along the path in which no phase shifter is present. Figures 6 and 7 show the effect of changing the phase shift between the beams to π.

5. DIFFERENCES BETWEEN DE BROGLIE AND BOHM IN THE NONRELATIVISTIC, MANY-BODY CASE

5.1. Quantum Statistics: Two Particles in a Harmonic-Oscillator Potential

In order to illustrate the manner in which Bohm's theory works in the many-body case, and to bring out the difficulties associated with the de Broglie program, we present here a brief description of a system of two noninteracting particles moving in one dimension, both subject to a harmonic-oscillator potential.[15,16] We shall see that, after specifying the particle positions and the forces acting on them,[6] the motion of the system is not determined unless we also specify the initial wavefunction. The

[6] Along with particle momenta these initial conditions would be sufficient to determine the motion of the system according to classical mechanics.

wavefunction determines the momenta through Eqs. (11). It is the many-particle wavefunction that determines the additional quantum forces acting on and between the particles and hence, unlike classical potentials, we see that the quantum potential is not a pre-assigned function of position. The quantum state determines the motion of the particles in the system. Evidently this feature has no counterpart in classical physics.

The extension of the Bohm theory to the nonrelativistic many body case is straightforward. The essential equations—the guidance formulas—are

$$\begin{aligned} m_1 v_1 &= \nabla_1 S(1, 2) \\ m_2 v_2 &= \nabla_2 S(1, 2) \end{aligned} \tag{11}$$

with $\psi(1, 2) = R(1, 2)\, e^{iS(1,2)/\hbar}$. Evidently, the velocity of either particle many depend on the coordinates of both, and hence the theory is nonlocal.

Returning to our chosen example, we want to be able to discuss the motion of the two particles under those circumstances in which they are initially placed at separate locations in the harmonic-oscillator potential. To this end we construct two coherent wavepacket states, $\psi_a(x, t)$ and $\psi_b(x, t)$, and arrange these so that initially the overlap is very small. Here they are initially centered on opposite sides of the potential, at x_a and x_b, respectively and x_a is chosen to be equal to $-x_b$. As is well known, it is then possible to write three alternative two-particle wavefunctions, depending on particle distinguishability and symmetry;

$$\phi_{MB} = \alpha_{MB} \psi_a(x_1, t)\, \psi_b(x_2, t) \tag{12}$$

$$\phi_{BE} = \alpha_{BE}[\psi_a(x_1, t)\, \psi_b(x_2, t) + \psi_b(x_1, t)\, \psi_a(x_2, t)] \tag{13}$$

$$\phi_{FD} = \alpha_{FD}[\psi_a(x_1, t)\, \psi_b(x_2, t) - \psi_b(x_1, t)\, \psi_a(x_2, t)] \tag{14}$$

where the α's are the normalization coefficients.

All three wavefunctions evolve deterministically and locally in the configuration space spanned by x_1 and x_2. The evolution of the probability density with time, for ϕ_{MB}, is shown in Fig. 8. The initial and final forms for the probability density for ϕ_{BE} and ϕ_{FD} are identical and are shown in Fig. 9. The forms of the probability density, for ϕ_{BE} and ϕ_{FD}, when the two initial packets in configuration space completely overlap, are shown in Figs. 10 and 11, respectively. We see that the two components of the wavefunctions given in (13) and (14) form initially separated packets in configuration space, which subsequently overlap, each producing an interference pattern. The difference between the phases of these two patterns, for

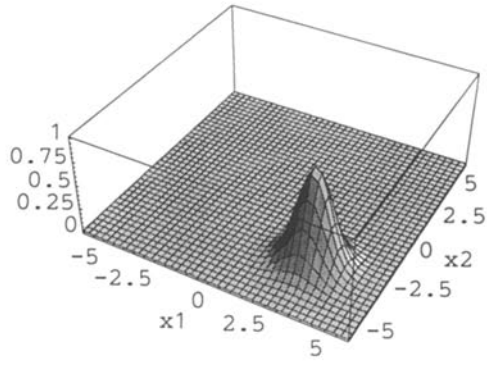

(a)

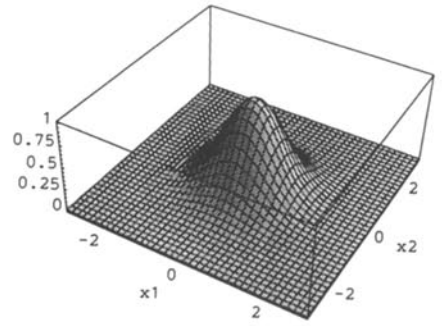

(b)

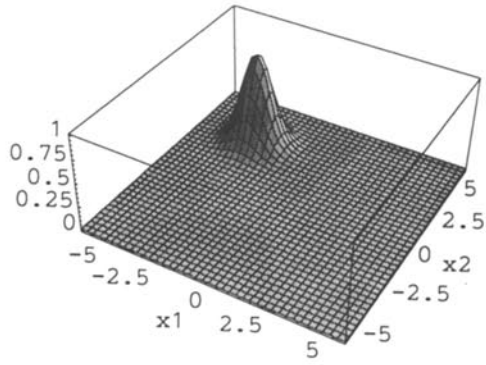

(c)

Fig. 8. The evolution of the configuration-space probability density for ϕ_{MB}.

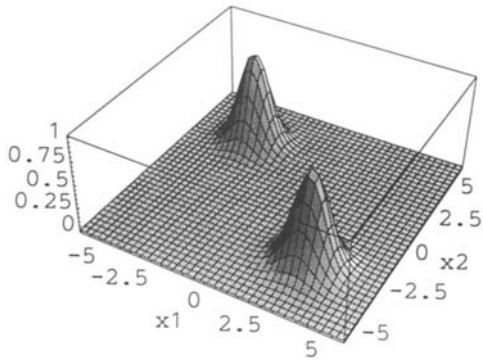

Fig. 9. The initial and final form for the configuration-space probability density for ϕ_{BE} and ϕ_{FD}.

ϕ_{BE} and ϕ_{FD}, is π.[7] Figures 12, 13, and 14 show the configuration space-time trajectories for ϕ_{MB}, ϕ_{BE}, and ϕ_{FD}, respectively. The individual particle trajectories are given by projecting the configuration-space trajectories onto the individual particle axes. In Figs. 15–17 we show a set of real space trajectories associated with the configuration space trajectories; for clarity we just plot those for which $x_1 = 2.5$ while $x_2 = -2.5$, -3.0, and -3.5. Note that, for the wavefunctions ϕ_{BE} and ϕ_{FD}, the specification of the initial position of a given particle is not sufficient to determine its motion. Figures 16 and 17 show that the trajectory of particle one splits

[7] Indeed, one could put $x_1 \to x$ and $x_2 \to y$ and view the evolution as that of a single-particle two-dimensional superposition wavefunction.

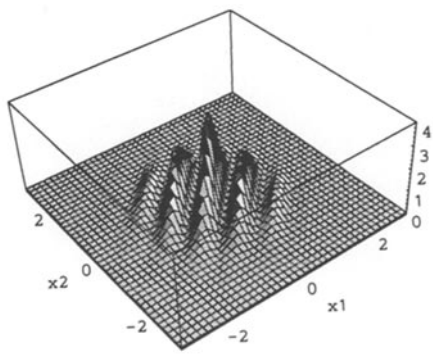

Fig. 10. The configuration-space probability density for ϕ_{BE}, when the wavepackets in configuration space completely overlap.

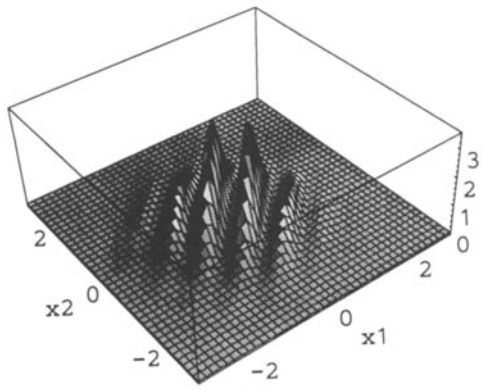

Fig. 11. The configuration-space probability density for ϕ_{FD}, when the wavepackets in configuration space completely overlap.

into three in the region where the wavepackets overlap. Which actual trajectory particle one occupies, in a given case, depends on which trajectory particle two follows; that is to say which is the corresponding configuration space trajectory. This is a general feature of Bohm's theory; which trajectory is actually realized, in a particular instance for a given particle, depends not only on its own initial position, but also on the initial positions that occur for the other particles, the initial configuration-space wavefunction, and the Hamiltonian of the system. These global dependen-

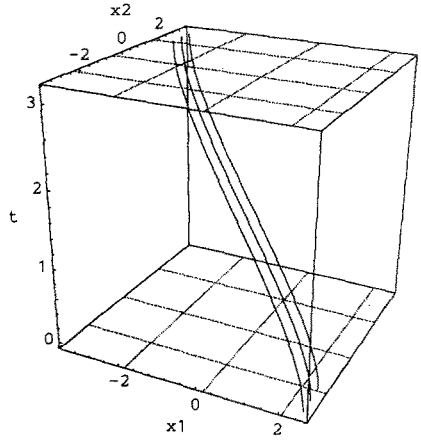

Fig. 12. Configuration space/time trajectories for ϕ_{MB}.

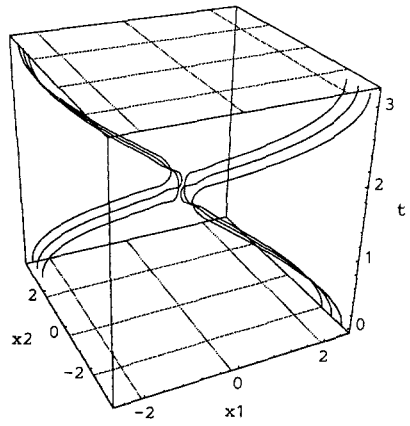

Fig. 13. Configuration space/time trajectories for ϕ_{BE}.

ces ensure that the Bohm theory is naturally both contextual and nonlocal. Since the theory has these features, the major no-hidden-variables theorems do not apply.[17]

The particle trajectories are thus nonlocally correlated, and this nonlocal correlation may be accounted for, in real space, by the action of the nonlocal quantum potential. In this case it can be seen that, in the Bohm's theory, nonlocality only arises when the system's wavefunction is not factorizable. It can also be seen that when ψ_a and ψ_b do not overlap, the

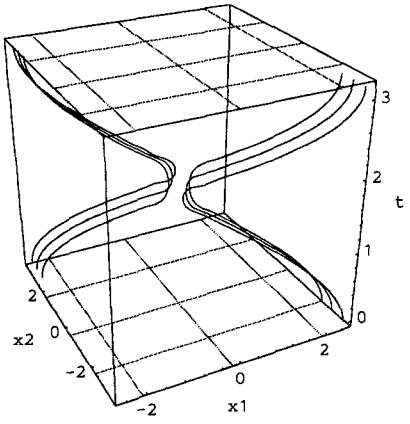

Fig. 14. Configuration space/time trajectories for ϕ_{FD}.

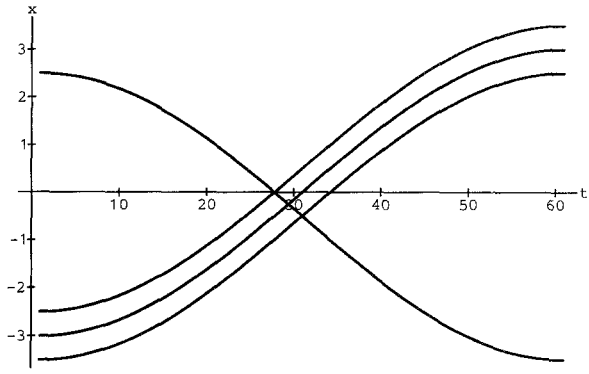

Fig. 15. Trajectories in real space for ϕ_{MB}, with $x_1 = 2.5$, $x_2 = -2.5$, -3.0, and -3.5, at $t = 0$.

particle trajectories develop locally. Thus, in this situation, Bohm's theory attributes nonlocality only in those circumstances in which it is usually not possible to say that the particles are separated.

5.2. Waves in Real Space?

The Bohm theory works, in the many-particle case, using a configuration-space wavefunction and not with individual-particle waves in three-dimensional space. One could introduce such waves in three-dimensional space by considering a section through the system configuration-space wavefunction, defined by the actual coordinates of all the particles except the one under consideration. This wavefunction, so defined, would then

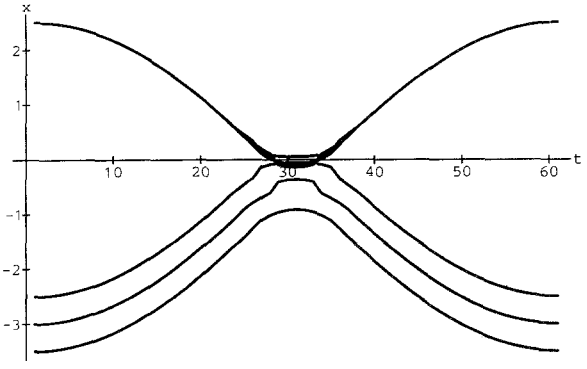

Fig. 16. Trajectories in real space for ϕ_{BE}, with $x_1 = 2.5$, $x_2 = -2.5$, -3.0, and -3.5, at $t = 0$.

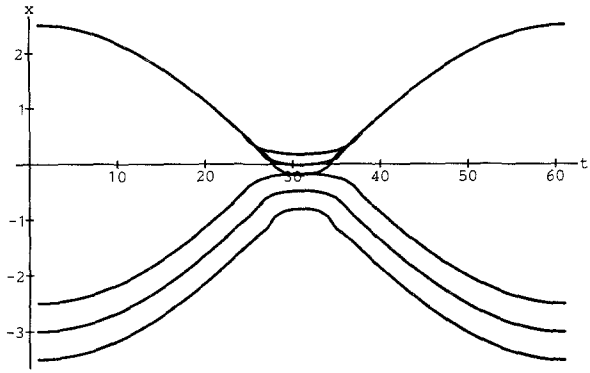

Fig. 17. Trajectories in real space for ϕ_{FD}, with $x_1 = 2.5$, $x_2 = -2.5$, -3.0, and -3.5, at $t = 0$.

evolve in a nonlocal and nonlinear manner; however, such a construction could only be performed in practice, *a posteriori*. The main point is that if one insists that both particles and waves must be in three-dimensional space, as did de Broglie, then it is possible to do so; but the price to be paid is that the waves will evolve both nonlocally and nonlinearly. Selleri *et al.* wish to define waves with just these properties ("Selleri–de Broglie" waves). They postulate that these waves exist in three-dimensional space and also insist that the equation they obey should be local. In this case, of course, the predictions produced by their theory will not reproduce those of quantum mechanics.

6. RELATIVISTIC FERMION SYSTEMS

In the following three sections we present the extension of the approaches of Bohm and de Broglie to the relativistic regime. In this section relativistic fermions are discussed and, in Secs. 7 and 8, the situation for bosons is considered. As far as relativistic fermion systems are concerned, both de Broglie[2] and Bohm[18] generalize their approaches to the Schrödinger equation to include the Dirac equation, in a straightforward manner. Bohm does not develop a full Hamilton–Jacobi type description for the Dirac equation—he simply defines a guidance formula, which is the approach followed here; whereas de Broglie does develop the relativistic Hamilton–Jacobi approach.

In this section some simple illustrative examples are used to bring out the interpretation of spin angular momentum in Bohm's approach to the single-particle Dirac equation. We first consider single plane waves and

note the absence of a spin current. Then the manner in which the spin current becomes apparent is examined for the case in which a wave packet solution is formed.

6.1. Dirac Trajectories

From the single particle Dirac equation,[8]

$$(i\partial\!\!\!/ - m)\psi = 0 \tag{15}$$

where Feynman "slash" notation,

$$a\!\!\!/ \equiv a^{\mu}\gamma_{\mu}$$

is used, and γ_{μ} are the usual Dirac matrices, it follows that there is a conserved current density, whose time component is positive definite. It is defined by

$$j^{\mu} = \bar{\psi}\gamma_{\mu}\psi \tag{16}$$

and

$$\partial_{\mu} j^{\mu} = 0 \tag{17}$$

where $\bar{\psi} \equiv \psi^{\dagger}\gamma^{0}$. Bohm[18] defines the velocity of the particle as

$$\mathbf{v} = \frac{\mathbf{j}}{j^{0}} = \frac{\bar{\psi}\gamma\psi}{\psi^{\dagger}\psi} \tag{18}$$

It is well known that the Dirac current can be decomposed into two parts, according to the Gordon decomposition. One part is associated with motion associated with a gradient field, while the other is a non-zero-curl circulatory (or spin) contribution. In the Bohm picture, this leads to the idea of the Dirac electron as a point-particle following a trajectory which has an overall translatory component and an additional circulation. Thus, in this approach spin is not an intrinsic property thought to arise from the rotation of an extended particle about its axis, as proposed in the application of the causal interpretation to the Pauli equation by Bohm, Schiller, and Tiomno.[13] The model proposed for the Dirac equation can also be applied to the Pauli equation, considered as a low velocity limit of the Dirac equation.[19]

[8] In all that follows, $\hbar = c = 1$.

For the purposes of illustration, only positive energy solutions (and superpositions thereof) of the free, single-particle Dirac equation will be considered.

6.1.1. Plane Wave Solutions. Positive-energy, plane-wave solutions of the Dirac equation, of wavenumber **k** and with an energy E, can be written using the usual four-vector notation

$$\psi(x) = e^{-ik\cdot x} u^{(\alpha)}(k) \tag{19}$$

where

$$u^{(1)} = \frac{1}{\sqrt{2m(E+m)}} \begin{pmatrix} E+m \\ 0 \\ k_3 \\ k_1 + ik_2 \end{pmatrix}$$

and

$$u^{(2)} = \frac{1}{\sqrt{2m(E+m)}} \begin{pmatrix} 0 \\ E+m \\ k_1 - ik_2 \\ -k_3 \end{pmatrix}$$

The two solutions, $u^{(1)}$ and $u^{(2)}$, represent plane waves travelling in the direction **k**, with spin up and spin down, respectively, along a z axis. It is readily shown that for plane waves the guidance condition (18) yields

$$\mathbf{v} = \frac{\mathbf{k}}{E} \tag{20}$$

for either $u^{(1)}$ or $u^{(2)}$. It can be seen by inspection that $v \leqslant 1$ (recall that $E^2 - \mathbf{k}^2 = m^2$). Hence the velocity of the Dirac particle will always be less than or equal to the speed of light, for plane waves. Evidently a Schrödinger[3] particle,[9] for which $v = k/m$, is not limited to a velocity less than c.

For a plane wave, then, the velocity term contains only a translational component and no circulation. These results may at first seem surprising since a Dirac particle, with a plane wavefunction and definite spin in some direction, actually has no spin component to its motion at all. Yet plane was are an abstraction, and a careful analysis of the process of measure-

[9] Which is also associated with a positive-energy plane wave.

ments of a spin component, using a Stern–Gerlach (SG) apparatus, shows that consistency with the usual results of quantum mechanics is obtained. In order for the SG apparatus to provide an unambiguous result, the quantum state must have the form of a spatially limited packet, which is achieved by the presence of a suitable slit at the entrance to the SG field. The interaction with the inhomogeneous magnetic field in the SG device then imparts an opposite momentum impulse to each of the components, $u^{(1)}$ and $u^{(2)}$ (assuming the SG to be aligned along the z-direction). If the two eigenstates of the spin are to separate spatially, it is necessary that the two packets separate more rapidly than they spread. This would not be possible for a single electron, but if the electron were an outer electron of a silver atom, then the large associated mass would ensure a spreading which was slower than the separation of the packets. After interaction with the SG field, the quantum state consists of two spatially separated packets, each associated with one component of the spin.

The form of the velocity will now be considered, along with the associated trajectories for laterally limited solutions obtained by superposition of solutions (19). de Broglie[2] demonstrates, using the example of Wiener fringes, that superpositions of waves in interference regions yield superluminal velocities near the interference minima. This occurs not only in the nonrelativistic theory, but also in his approach to the Klein–Gordon equation (see Sec. 8). In the Dirac theory, the velocity is always subluminal.

6.1.2. Superposition of Plane Waves. Consider the following solution to Dirac's equation

$$\psi(x) = e^{-ik\cdot x}u^{(1)}(k) + Re^{-ik'\cdot x}u^{(1)}(k') \tag{21}$$

consisting of a superposition of two plane waves, with a ratio of amplitudes R, both with spin along the z (or 3) axis and travelling in directions $\mathbf{k}$ and $\mathbf{k}'$.

The Gordon decomposition of the current density yields

$$m\mathbf{j} = (1 + r\cos\theta)\mathbf{k} + (R^2 + r'\cos\theta)\mathbf{k}' + (r\sin\theta\mathbf{k} - r'\sin\theta\mathbf{k}') \times \hat{\mathbf{e}}_3 \tag{22}$$

where $\theta = (k - k')\cdot x$, $r = R[(E' + m)/(E + m)]$, $r' = R[(E + m)/(E' + m)]$ and $\hat{e}_3$ is the unit vector parallel to the z-axis. The probability density is also easily calculated as

$$m\rho = mj^0 = E + R^2E' + \frac{R\cos\theta}{\sqrt{(E'+m)(E+m)}}(\mathbf{k}\cdot\mathbf{k}' + (E' + m)(E + m)) \tag{23}$$

According to (18), the velocity has two components—one translational and the other of "spin." In this case, again, the spin term is not associated with any rotational motion, but is linear in a direction perpendicular to $(\mathbf{k}\cdot\mathbf{k}')$ and $\hat{\mathbf{e}}_3$. For the special case where $\mathbf{k}=-\mathbf{k}'=k_3\hat{\mathbf{e}}_3$ and hence $E=E'$, the Dirac velocity is given by

$$\mathbf{v}=\frac{\mathbf{j}}{\rho}=\frac{(1-R^2)k_3\hat{\mathbf{e}}_3}{(1-R^2)E+2mR\cos\theta} \tag{24}$$

It is interesting to note that the density has no nodes when $R=1$, and that the velocity is (as it must be) subluminal, whereas for $\psi(x)=e^{-i(Et-k_3z)}+Re^{-i(Et+k_3z)}$ the Schrödinger guidance formula[3] yields

$$\mathbf{v}=\frac{1}{m}\frac{\partial S}{\partial z}=\frac{(1-R^2)\,k_3\hat{\mathbf{e}}_3}{m(1+R^2+2R\cos\theta)} \tag{25}$$

In the Schrödinger case, the velocity can become arbitrarily large in the regions where $\rho\to 0$ (if $R=1$, ρ can be zero). This, of course, is not problematic in a nonrelativistic theory. Even in the low-energy limit of the Dirac equation, where relativistic effects may be thought to be unimportant, it can be seen that the relativistic corrections to ρ, evident in the denominator of (24), play an important role in ensuring subluminal velocities by their alteration of the behavior of this equation in the limit. Thus it is important, from the computational point of view, to use the Dirac theory for trajectory calculations even in cases for which relativistic effects are usually considered unimportant.

Consider now the case in which a particle moves in the z-direction, but has a wavefunction limited in the x-y plane. Ideally, a single wavepacket solution should be used, but here a superposition of just four plane waves is considered.

$$\psi(x)=\sum_{n=1}^{4} e^{-ik^{(n)}\cdot x}u^{(1)}(k^{(n)}) \tag{26}$$

This produces an infinite rectangular array of packets in the x-y plane. For the purposes of illustration it is assumed that the energy, $E=k_0^{(n)}=2$, is the same for each wave, along with the z-component of the wavevector of each wave, $k^{(n)}$, which is taken to be zero. The other components of the wavevectors are taken to be $k_1^{(1)}=k_2^{(1)}=1$, $k_1^{(2)}=-k_2^{(2)}=1$, $k_1^{(3)}=-k_2^{(3)}=-1$, and $k_1^{(4)}=k_2^{(4)}=-1$. Figure 18 shows that the form of the probability density in the x-y plane is time-independent and possesses an infinite number of localized peaks. The velocity, which is always in the x-y plane, can be calculated from (18) and integrated numerically to give a set of tra-

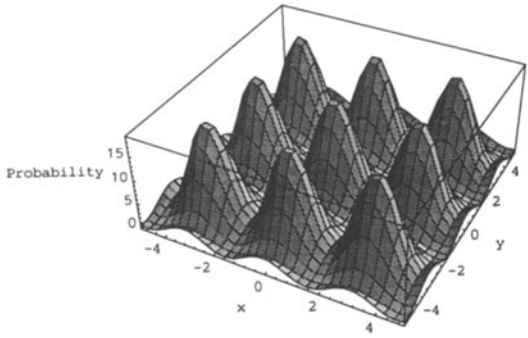

Fig. 18. Probability density, $\Psi^{\dagger}\Psi$, according to the Dirac equation, for a superposition of four plane waves travelling in each sense of two perpendicular axes in the x-y plane.

jectories. A set of trajectories is shown which has different initial positions along the x-axis and which is associated with just one of the probability density peaks.

Figure 19 shows a set of trajectories for the case in which the z-component of each wavevector is zero. It shows that the particles perform a circulatory motion. Figure 20 shows how the trajectories evolve in space/time.[10] In this case there are a set of nodal lines for the velocity, forming a grid in the x-y plane.

It has been shown that, insofar as the Dirac equation can be treated as a single-particle equation, Bohm's theory gives a consistent interpreta-

[10] Figure 19 is the view from the "top" of this figure.

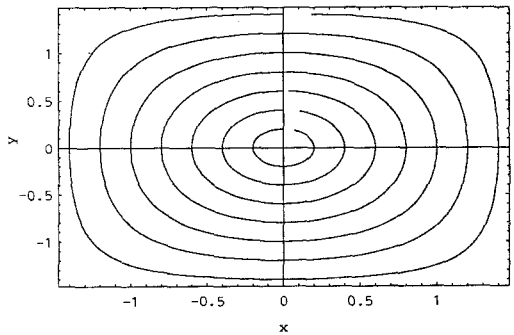

Fig. 19. A set of trajectories associated with the superposition of four plane waves travelling in each sense of two perpendicular axes in the x-y plane.

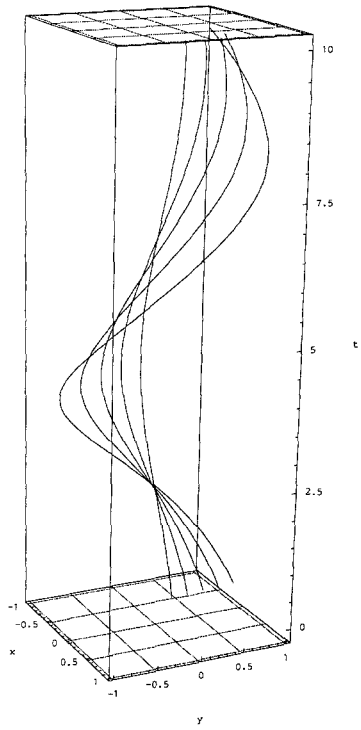

Fig. 20. Evolution in time of the trajectories associated with the superposition of four plane waves travelling in each sense of two perpendicular axes in the x-y plane.

tion in terms of particle trajectories. Bohm and Hiley have indicated[19] that the extension to the many-particle case can be carried out consistently, and they have also discussed the question of relativistic invariance within this approach. The application of the two-particle Dirac equation to the EPR spin-correlation experiment will be discussed by us, in detail, in a forthcoming publication.

7. BOHM'S QUANTUM FIELD THEORY FOR BOSONS

Bohm first outlined the essential details of this approach to quantum theory in 1952, in the appendix of his paper "A suggested interpretation of the quantum theory in terms of hidden variables II."[3] More recently,

further details of this approach have been given by Bohm, Hiley, and Kaloyerou, in the context of a scalar field $\phi(x, t)$.[20]

In Bohm's quantum field theory (BQFT), the field is always well defined and it evolves according to a deterministic, but nonlinear and nonlocal, field equation. Given the initial form of the field, the super-wavefunction, $\Psi(\phi)$, and the Hamiltonian, BQFT provides a continuous and deterministic description of the development of the field, $\phi(x, t)$. As in the case of quantum particle systems, the causal interpretation of quantum fields shares the observed results of the orthodox theory, but has the advantage of possessing a well-defined model of individual physical systems in all contexts and, of course, the theory does not depend on the existence of an observer for its interpretation. The consistency of the predictions of the causal interpretation of quantum fields with those of the usual theory can be demonstrated through a discussion of the measurement process. This process is essentially the interaction of the field with matter, and it is also in this situation that the particle nature of the field is observed.

Here we shall briefly review the framework of the approach of Bohm *et al.* for the case of a real, massless scalar field, $\phi(x, t)$, confined to a one-dimensional cavity, extending between $x = 0$ and $x = L$ (we shall put $\hbar = 1$ and $c = 1$). The boundary conditions require that the field be zero at $x = 0$ and $x = L$, so that the normal modes of the field in this cavity are

$$\phi_k(x) = \left(\frac{2}{L}\right)^{1/2} \sin kx \tag{27}$$

An arbitrary state of the field may then be written as

$$\phi(x, t) = \left(\frac{2}{L}\right)^{1/2} \sum_k q_k(t) \sin kx \qquad \left(k = \frac{n\pi}{L}, n = 1, 2, \ldots\right) \tag{28}$$

As is well known, the classical equation of motion for each coordinate, q_k, of the field is

$$\frac{\partial^2 q_k}{\partial t^2} + k^2 q_k = 0 \tag{29}$$

This is the equation of motion for a harmonic oscillator of coordinate q_k, frequency $\omega = k$, and mass $m = 1$, so the field can be represented by an infinite set of harmonic oscillators each obeying Eq. (29). The set of oscillators is quantized by the introduction of a Schrödinger equation, termed by Bohm *et al.* the super-Schrödinger equation:

$$i\hbar \frac{\partial \Psi}{\partial t}(\ldots, q_k, \ldots, t) = \frac{1}{2} \sum_k \left(- \frac{\partial^2}{\partial q_k^2} + k^2 q_k^2 \right) \Psi(\ldots, q_k, \ldots, t) \tag{30}$$

It is this equation which governs the behavior of all field oscillators.

The usual interpretation of the wavefunction, $\Psi(..., q_k, ..., t)$, is simply that $|\Psi|^2$ gives the probability density for "finding" a particular set of q_k's. To obtain a causal interpretation for the quantized field we write, just as is done for the case of quantum particle systems,

$$\Psi(..., q_k, ..., t) = R(..., q_k, ..., t) \exp(iS(..., q_k, ..., t)) \tag{31}$$

where R and S are real and Ψ is a function of a configuration space of infinite dimensions, which is spanned by all the oscillator coordinates. One finds, by substituting this form of Ψ into the Schrödinger equation, that

$$\frac{\partial S}{\partial t} + \frac{1}{2}\sum_k \left(\left(\frac{\partial S}{\partial q_k} \right)^2 + k^2 q_k^2 \right) - \frac{1}{2}\sum_k \frac{1}{R_k} \frac{\partial_k^2 R}{\partial q_k^2} = 0 \tag{32}$$

$$\frac{\partial P}{\partial t} + \sum_k \frac{\partial}{\partial q_k} \left[P \frac{\partial S}{\partial q_k} \right] = 0 \tag{33}$$

where $P = |\Psi|^2$. Taking Eq. (32) as the Hamilton–Jacobi equation for the field, $\phi(x, t)$, implies that $\partial S/\partial q_k$ is the rate of change of q_k. However, there is an additional energy term, not present in the classical equation, which is termed the super-quantum potential

$$Q = -\frac{1}{2}\sum_k \frac{1}{R_k} \frac{\partial_k^2 R}{\partial q_k^2} \tag{34}$$

If $\partial S/\partial q_k$ is taken as the rate of change of the mode coordinate q_k, then Eq. (33) expresses the conservation of probability. If it is assumed that, at some point in time, the probability density $P = |\Psi|^2$ gives the actual distribution of the coordinates q_k in an ensemble, then P will continue to give the distribution for all subsequent times.

In general the field itself, $\phi(x, t)$, is the "hidden variable" (or beable), but within this normal mode formulation the mode coordinates, ..., q_k,..., may be thought of as the "hidden variables." Each q_k has a well-defined value and therefore, according to Eq. (28), the field $\phi(x, t)$ is also well defined. Each coordinate, q_k, evolves according to

$$\frac{\partial q_k}{\partial t} = \Pi_k(t) = \frac{\partial S}{\partial q}(..., q_k, ..., t) \tag{35}$$

so that its motion is determined in the configuration space spanned by all the cavity coordinates, ..., q_k,.... Given the initial values of the mode coordinates (the set of which is referred to collectively as the initial "system point" in configuration space) and the initial wavefunction for the system, $\Psi(..., q_k, ...)$, the trajectory of the system point is determined, and it is this trajectory which determines the evolution of the field $\phi(x, t)$ in real space.

Evidently, in this approach there are no photon trajectories and the "photon" itself is simply an excitation of a field mode. Instead there are well-defined quantum fields which evolve continuously and deterministically, according to Eq. (35). The particle-like aspects of the field arise as a result of the influence of the super-quantum potential on the evolution of the system point, as the field interacts with matter. Bohm, Hiley, and Kaloyerou have discussed this in a general way, and two of us (M.M.L. and C.D.) have carried out detailed modelling for cavity fields.[21]

Next we take the discussion further, in order to explore the nonlocality involved in the anticorrelation between two atoms interacting with a single photon field. At first sight it would seem that a theory based on boson trajectories would give a simple and intuitive description of the anticorrelation, since a localized photon on a trajectory could only be in the vicinity of one detector (atom). It is fascinating to see that the observed results can be recovered deterministically and causally using extended, but well-defined fields.

7.1. Anticorrelation between Two Atoms in a One-Photon Field

In this section we illustrate how Bohm's causal field theory can provide a deterministic account of the results of the experiment proposed by Ghose *et al.*, which is described in Sec. 9.3 and illustrated in Fig. 21. The key feature of this experiment is the anticorrelation observed between the firing of two detectors, C_1 and C_2, placed in a one-photon field.

The energy of a quantum field, at a particular point in space, is measured by allowing the field to interact with a detector (i.e., matter) placed at that point. This interaction creates a correlation between the

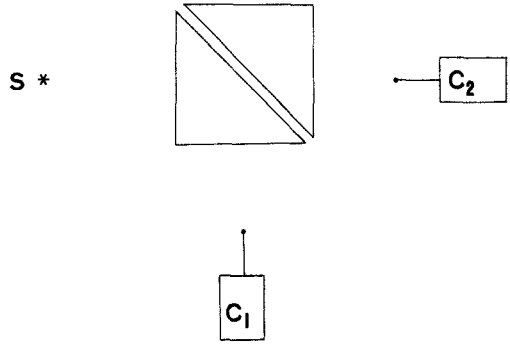

Fig. 21. Experimental arrangement of the anticorrelation experiment of Ghose *et al.*

state of the field and the state of the matter, allowing us to deduce the former, at a particular moment in time, from the result of a measurement performed upon the latter.[11] Measurement of the energy of a quantum field yields discrete spectra of values; for example, photon counts are detected by a photomultiplier tube, placed within a quantum field.

A simple model of the detection of a one-photon field is provided by the example of a single-mode field, which is coupled for a certain period of time to a two-level atom, with a subsequent observation of the state of the atom. This observation is made through the use of a measurement of the atomic momentum. If the momentum of the atom corresponds to the excited state, then the field is assumed to have transferred its quantum of energy to the atom. Alternatively, it the momentum of the atom corresponds to the ground-state eigenvalue, the field is assumed not to have lost any energy. Extending this idea further, the experiment of Ghose *et al.* can be modelled by using a system of two identical two-level atoms both coupled, for a period of time, to a single-mode one-photon field in a cavity (but not coupled to each other). After the period of interaction, each atomic electron is released from its confining potential and the time taken for each to reach a fixed detector is observed. From the momentum measurement of either atom, the state of the field may be deduced.

An atom is represented in this model by a single electron confined within an infinite well of width $L = \pi$, and the field mode is represented by a harmonic oscillator of mass 1. Here we ignore the parts of the super-wavefunction which represent all other field modes, since these vacuum state modes are not entangled with the mode coupled to the atoms and so develop independently from it. The angular frequency associated with the field-mode, ω, is taken to be precisely that frequency associated with the transition between the ground level and one of the excited levels of the infinite well, enabling us to treat each atom as a two-level system. The two atoms are coupled to the field by interactions of the form

$$V_i = q \sin(\kappa x_i + \phi_i) \tag{36}$$

where atoms 1 and 2 are labelled by $i = 1$ and 2, respectively. In Eq. (36), q is the coordinate of the field mode, κ is the wavevector of the mode, and ϕ_1 and ϕ_2 are phases which depend on the position of each atom in the cavity. Although the atoms are considered to be in different regions of the cavity, it is assumed that the dimensions of the atoms, and their separation, are small in comparison with the wavelength of the field and that the sizes of the interaction of each atom with the field are approximately equal,

[11] Two of us (C.D. and M.M.L.) have already modelled the measurement of energy for matter interacting with a classical field.[14]

allowing us to put $\phi_1 = \phi_2 = 0$. Without the presence of the interaction, the field–matter system is triply degenerate, and the effect of the coupling of the atoms to the field can be found using degenerate perturbation theory. If the ground and excited-state wavefunctions of the two atoms are atoms are denoted by $\psi_0(x_{1,2})$ and $\psi_1(x_{1,2})$, respectively, and the ground and first-excited states of the mode oscillator are represented by $\theta_0(q)$ and $\theta_1(q)$, then the three degenerate levels are

$$U_1 = \theta_1(q)\,\psi_0(x_1)\,\psi_0(x_2)$$
$$U_2 = \theta_0(q)\,\psi_1(x_1)\,\psi_0(x_2)$$
$$U_3 = \theta_0(q)\,\psi_0(x_1)\,\psi_1(x_2)$$

If the system is in the state $U_1(x_1, x_2, q)$ at $t = 0$, then the subsequent development of the system wavefunction during the period of interaction is given, from degenerate perturbation theory, by

$$\Psi(x_1, x_2, q, t) = U_1(x_1, x_2, q)\cos \Omega t - \frac{i}{\sqrt{2}} \sin \Omega t [U_2(x_1, x_2, q) + U_3(x_1, x_2, q)] \quad (37)$$

where Ω depends on the overlap integrals between the unperturbed states, for the interaction V_i. When Ωt is an integer multiple of π (case A), the system is entirely in the state U_1. This is normally interpreted as corresponding to an excited field and two unexcited atoms since, at this time, a measurement of the energy of each atom will yield the ground-level eigenvalues. When Ωt is a half-integer multiple of π (case B), the system is in a superposition of the states U_2 and U_3. This is usually interpreted as corresponding to a de-excited field and either atom 1 or atom 2 being excited, since if a measurement of momentum is performed on both atoms at this time, one of the atoms (the probability of it being atom 1 or atom 2 is equal) will be observed as having the ground level energy, while the other will have the momentum eigenvalue corresponding to the excited state. The wavefunction of the two atoms, for these values of time, is

$$\Psi(x_1, x_2, q, t) = \frac{\pm i}{\sqrt{2}} [U_2(x_1, x_2, q) + U_3(x_1, x_2, q)] \quad (38)$$

which is an entangled state involving the two separated atomic systems, i.e., the type of wavefunction required to observe EPR-type correlations.

For all other values of t, the system wavefunction is a superposition of the two states corresponding to cases A and B, and observations associated

with either case are made with probabilities that vary as a function of time, as given by Eq. (37). For these values of time, it is not possible, in the usual approach, to give any description of the behavior of the field or the atoms. The most complete description of the quantum system, which can usually be given, is in terms of the probability of a quantum of energy being detected at a given position and time, and this is provided by the system wavefunction.

The causal interpretation of quantum fields is able to provide, in addition to this statistical description, a precise account of the development of a well-defined quantum field, along with a unique trajectory for the matter with which the field is interacting, and it can provide this for all times—before, during, and after measurement. As in the usual theory, the description of the causal theory is in terms of the field–matter wavefunction, which exists in the configuration space spanned by x_1, x_2, and q, but unlike the usual theory it assigns a precise value for the field coordinate and the positions of the atomic electrons.

The coordinates of the system, x_1, x_2, and q, are collectively referred to as the "system point." The probability of the system point possessing a certain value, at any time t, is given by the usual probability density $P(x_1, x_2, q, t) = |\Psi(x_1, x_2, q, t)|^2$ of quantum mechanics, which usually only provides the probability of measuring this value.

We consider a period of coupling between the field and the two atoms of $\pi/2\Omega$, at the end of which the state of the system is a product of a field wavefunction and an entangled wavefunction for the two atoms. Figure 22 shows how the probability density varies between the time period $t = 0$ and $t = \pi/2\Omega$, as a function of the variables x_1, x_2, and q (regions of probability density above a certain value are filled with dots). The excited level of the two-level atoms is taken to be the first-excited state of the infinite well, as the use of this state produces the least complicated motion. At $t = 0$, there are two regions of high probability density, localized around $(x_1, x_2, q) = (1.57, 1.57, \pm 0.56)$, respectively, and at $t = \pi/2\Omega$, there are two maxima of probability, centered about (0.79, 0.79, 0) and (2.36, 2.36, 0).

Using Eqs. (5) and (35), the trajectory for a given initial system point may be calculated. Figures 23a and 23b show sets of possible trajectories for the time period $t = 0$ to $\pi/2\Omega$. In Fig. 23a, there is a set of six trajectories, which divide into group (i) trajectories, with an initial value of q of 0.46 and group (ii) trajectories, with an initial value for q of 0.66. Within each group there are three initial values for (x_1, x_2), and these are (1.47, 1.47), (1.47, 1.67), and (1.67, 1.47). The figure clearly shows that group (i) trajectories enter the area occupied by one of the final maxima of probability density, whereas group (ii) trajectories enter the other maximum. Due to the symmetry of the system, the set of trajectories, with their initial

system points centered about $(x_1, x_2, q) = (1.57, 1.57, -0.56)$, behaves in a very similar fashion, as shown by Fig. 23b.

The behavior of the quantum field and the two electrons, in real space, is given by the projection of the system point trajectory onto the axes, q, x_1, and x_2, respectively. Figure 24 shows the projection of the system trajectories of Fig. 23a onto the x_1 axis; this is identical to its projection

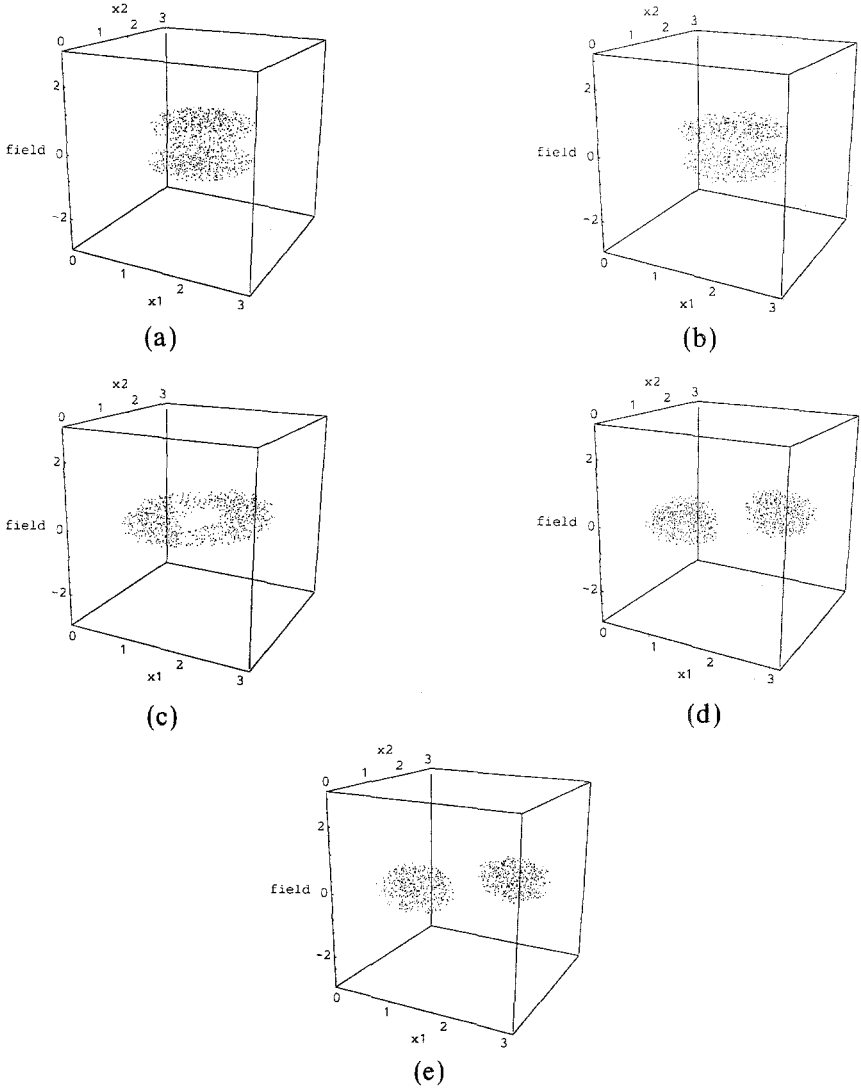

Fig. 22. Evolution of the probability density for two interacting with a single-mode field, between times $t = 0$ and $t = \pi/2\Omega$.

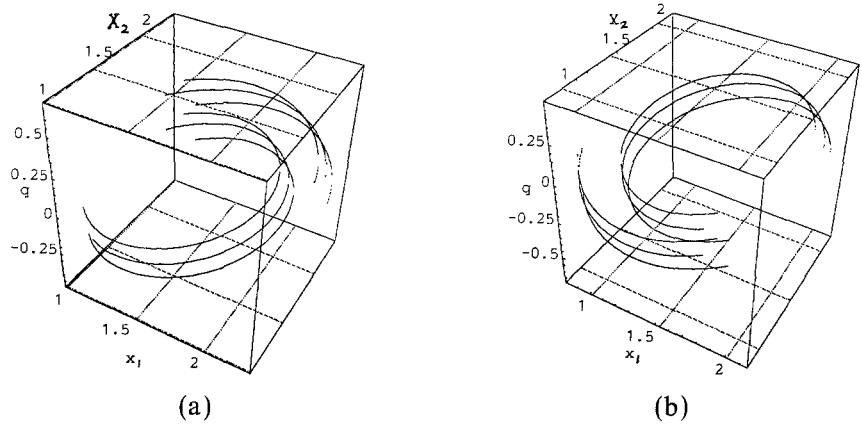

Fig. 23. Configuration-space trajectories, between times $t=0$ and $t=\pi/2\Omega$, for two atoms interacting with a single-mode field; with the system-point values initially centered about $(x_1, x_2, q)=(1.57, 1.57, 0.56)$ (a) (1.57, 1.57, −0.56) (b).

onto the x_2 axis. Figure 25 shows the projection of the configuration-space trajectories onto the q axis, and this shows that trajectories with the initial points (q, 1.47, 1.67) and (q, 1.67, 1.47) are identical to each other, but different from the trajectory with initial point (q, 1.47, 1.47). These projected trajectories demonstrate that the behavior of each part of the system depends not only on its own initial coordinate, but also on the initial coordinates of all other parts of the system, regardless of the separation between the parts, reflecting the explicit nonlocality of the theory.

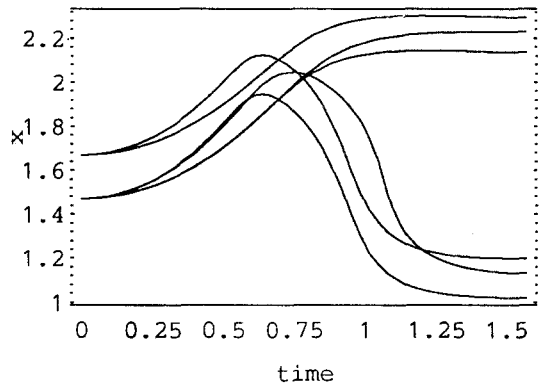

Fig. 24. Projection onto the x_1 (or x_2) axis, of the configuration-space trajectories, for two atoms interacting with a single-mode field, with the system-point values initially centered about (1.57, 1.57, 0.56).

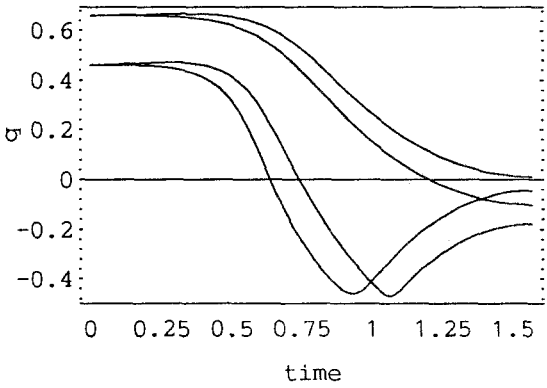

Fig. 25. Projection onto the q axis, of the configuration-space trajectories, for two atoms interacting with a single-mode field, with the system-point values initially centered about (1.57, 1.57, 0.56).

After the period of interaction, the field and the two atoms are decoupled and the final part of the detection process takes place; this is the performance of a momentum measurement on each atom. One way of observing atomic momentum is by removing the infinite potential containing the electron, which causes the spatial separation of the wavefunction into a superposition of orthonormal eigenfunctions of the atomic momentum. The position of the electron, after the spatial separation of the eigenfunctions, is correlated with the measured value of momentum. The decoupling and the removal of both atomic potentials occurs at time $t = \pi/2\Omega$, when the wavefunction is a product of two wavefunctions—one for the field and one for the two atoms. After this point in time, the development of the field is independent from that of the atoms, and the final part of the detection of the field quanta may be modelled using the two-atom entangled state alone, which at $t = \pi/2\Omega$ is

$$\psi\left(x_1, x_2, \frac{\pi}{2\Omega}\right) = \frac{-i}{\sqrt{2}}\left[\psi_1(x_1)\,\psi_0(x_2) + \psi_0(x_1)\,\psi_1(x_2)\right] \tag{39}$$

If the energies of the two atomic levels are of suitable relative magnitudes, then, after the removal of the infinite potentials, the different momentum-components of the two-atom wavefunction will separate, as was demonstrated in a previous paper[14] by two of us (C.D. and M.M.L.). In this paper, we modelled the measurement of the state of an electron confined within an infinite 1D potential well, undergoing a transition between its ground and third-excited states, using the nonrelativistic causal

theory. The transition was caused by an interaction with an unquantized field, at the resonant frequency for that transition.

The observed state of the electron (either the ground or the third excited) was deduced from a measurement of momentum, performed halfway through the transition, when the system wavefunction was a superposition of the ground and third excited states. On removing the infinite potential well, the wavefunction for the atom initially ran out in each of the directions, $+x$ and $-x$, and then separated into three wavepackets; two moving outwards from the center, associated with the higher-energy component, E_3, and the third (as yet unseparated) in the center, associated with the ground-state energy component, E_0, (see Fig. 26). The electron was guided by the quantum potential, so that, as the three packets

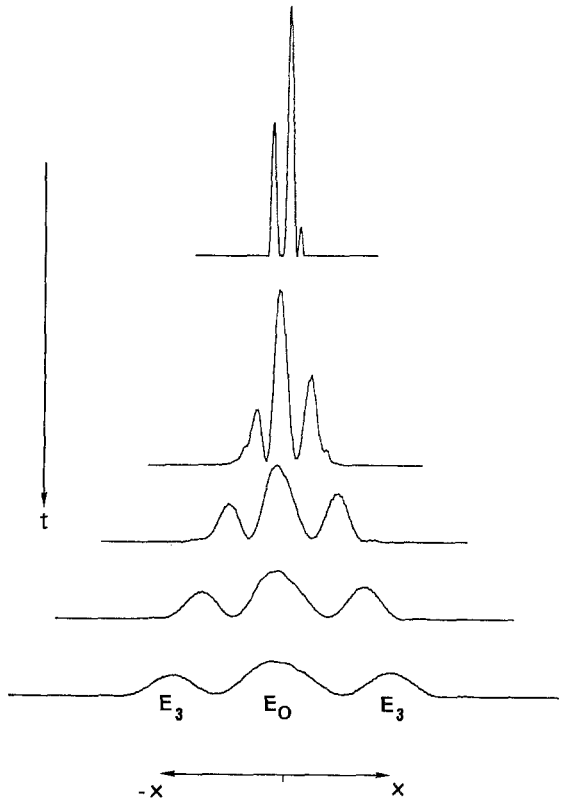

Fig. 26. Evolution of the probability density after the removal of the confining potential for a single two-level atom. The wavefunction is initially a superposition of the ground and third excited states of the infinite well.

separated, it was positioned within one of the packets and subsequently remained localized within that packet. The trajectory of the electron was shown to depend on its position at the point of the removal of the potential. A particle detector, placed some distance from the origin of the well, detected different times-of-flight for the electron, depending on which packet it eventually became associated with.

It is interesting to note that if the semiclassical treatment, given in Ref. 14, is extended to the case of two atoms interacting with a single-mode cavity field, then the quantum state of the atoms remains a simple product; no anticorrelation can be encompassed by the semiclassical description. Here, in the fully quantized description, the overall state of the two atoms becomes entangled through the interaction with the single-photon field.

In order to illustrate the momentum measurement, we now choose the upper atomic levels to be the third excited state of the infinite well (of energy E_3), rather than the first excited state, to ensure complete spatial separation of the eigenfunctions of momentum. Figure 27 shows the probability density for the two-atom entangled state, at the end of the period of interaction between the field and the atoms. The probability density not only represents the probability of the system particle being *detected* at a point (x_1, x_2), as in the usual interpretation of the theory, but here it also gives the probability of the electrons *being* at that point. We can deduce,

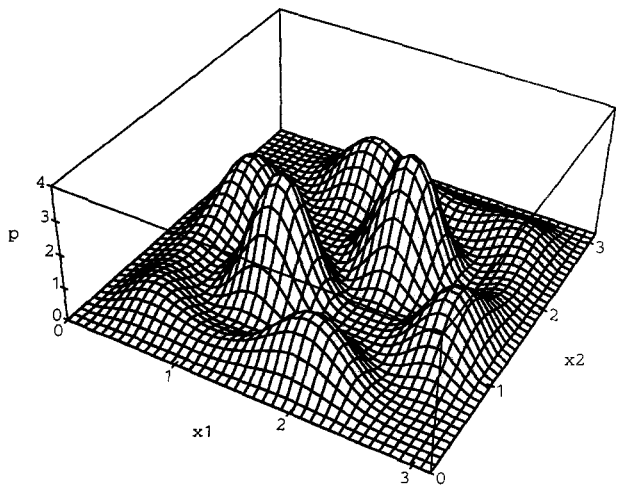

Fig. 27. Probability density for the two-atom entangled state at the end of the period of interaction with the single-mode field, at time $t = \pi/2\Omega$.

from the single two-level atom case, that the wavefunction of the two-atom system, some time after the removal of the infinite potentials, is given by

$$\chi(x_1, x_2, t) = -\psi_0(x_2, t)[\psi_1(x_1, t)^L + \psi_1(x_1, t)^R] - \psi_0(x_1, t)[\psi_1(x_2, t)^L + \psi_1(x_2, t)^R] \quad (40)$$

where L and R denote two spatially separated wavepackets, moving in opposite directions. This wavefunction has a probability density of the form

$$p(x_1, x_2, t) = [\psi_1(x_1, t)^L \psi_0(x_2, t)]^2 + [\psi_1(x_1, t)^R \psi_0(x_2, t)]^2 + [\psi_0(x_1, t)\, \psi_1(x_2, t)^L]^2 + [\psi_0(x_1, t)\, \psi_1(x_2, t)^R]^2 \quad (41)$$

Therefore, after the separation of the momentum wavepackets for each atom, the probability density for the two-atom system consists of four wavepackets, wp1, wp2, wp3, and wp4, each moving away from the origin, as shown in Fig. 28. This figure also shows the positions of four particle detectors (for instance, photographic plates); there are two for each atom, one for the positive component of momentum and situated along the positive axis, the other for the negative component, at the equivalent position along the negative axis. Atom 1 may be detected by either d_1 or D_1, depending on which wavepacket it becomes associated with, and atom 2 may be detected by d_2 and D_2, all detectors being situated an equal

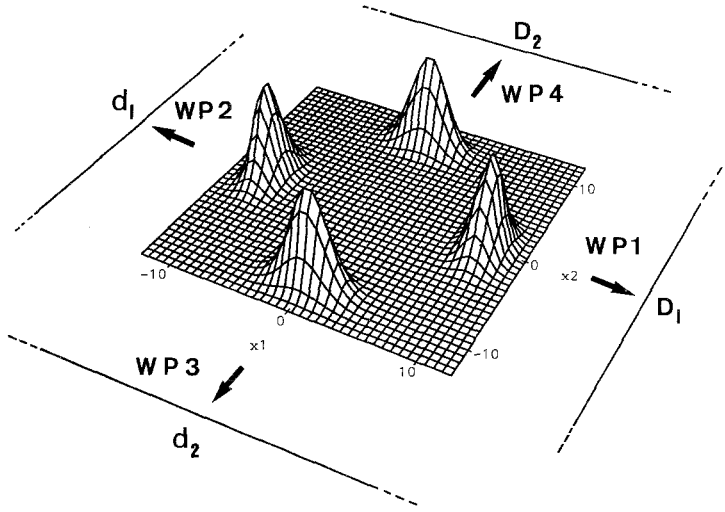

Fig. 28. Probability density for the two-atom system, after the spatial separation of the momentum eigenstates has occurred.

distance along their respective axis. Once the system point, (x_1, x_2), has become localized within one of the wavepackets, it must remain within that packet, since it cannot cross the regions of zero probability separating the different packets.

Of course, the system point may be localized within any one of the four wavepackets, but if it is localized, for instance, within wavepacket wp1, then the electron from atom 2 will not be detected, but atom 1 will eventually be detected by D_1, since wp1 remains localised around $x_2 = 0$, but travels along the positive x_1 axis towards D_1. If we examine the motion of the other three packets, we can see that the firing of detectors D_1 and d_1 is associated with no firing of the detectors for atom 2 and that the firing of D_2 and d_1 is accompanied by no firing of d_1 or D_1, i.e., anticorrelation is observed between the firing of the detectors for atoms 1 and 2.

In this section, we have given a causal description of the anticorrelation observed between two detectors in a one-photon field, using Bohm's quantum field theory for scalar massless bosons. In this picture, there is a well-defined motion for the quantum field, but no photon trajectories, a photon being just an excitation of a mode. So we have demonstrated that we do not need the concept of a photon-particle to described quantum field phenomena, only a precise form for the quantum field. The observation of field quanta is then due to observation of the quantized energy of the detector used to deduce the state of the field.

The behavior of the field may be found from the motion of the system point, which is determined by its initial value (i.e., the initial values of the dynamical variables of all parts of the system, regardless of their separation), and by the development of the system wavefunction. The behavior, in real space, of individual parts of the system can be found from the description in configuration space; this leads straightforwardly to a account of the nonlocal correlations between these parts.

8. RELATIVISTIC BOSON PARTICLE TRAJECTORIES?

In classical relativistic mechanics, a massive particle has a definite world line in space-time. Massless particles, with spin greater than zero, however, are only located on a two-dimensional null hyperplane[22,23] from which one could conclude that they are nonlocal objects (Penrose), or that classical mechanics is not sufficient to determine their worldlines.

Attempts to extend these results to a causal interpretation of relativistic quantum mechanics have led to problems, especially for bosons. Thus, as we have seen in Sec. 7, Bohm has proposed a purely field picture for bosons which is, however, causal; while de Broglie and Vigier have

maintained the possibility of a particle interpretation for both fermions and bosons. de Broglie has clearly laid out the problems for a scalar spin-zero boson, obeying the Klein–Gordon equation.[2] A Hamilton–Jacobi type equation can be derived by the usual substitution, $\psi = R\,e^{iS/\hbar}$, and leads to a relativistic generalization of Bohm's quantum potential, namely $-\hbar^2(\Box R/R)$, with four-momenta $\nabla_\mu S$ and a variable proper mass, M_0, defined by

$$M_0^2 = m^2 + \hbar^2 \frac{\Box R}{R} \tag{42}$$

In this interpretation it should be noted that the four-momenta are proportional to the conserved current vector, $j_\mu = R^2 \nabla_\mu S$. Unfortunately, as pointed out by de Broglie,[2] the simple case of two counter-propagating Klein–Gordon plane waves leads to superluminal velocities in some regions of space. The result is very counterintuitive, as remarked by J. Bell,[45] since the problem occurs no matter how small the relative amplitude of one of the waves. However, no contradiction with relativity is entailed since the variable proper mass goes to zero as the particle approaches the velocity of light; the velocity average over a wavelength is always less than c and any attempt to measure the superluminal velocities must entail a consideration of the propagation of energy whose velocity is always less than c.

The interesting alternative particle description, given by de Broglie[2] and Vigier,[24] involves modifying the metric tensor by a conformal transformation, $g_{\mu,\nu} \to (M_0/m)^2 g_{\mu,\nu}$, and showing that the trajectories are geodesic when this modified metric is used; when M_0^2 is negative, the role of the time and space axes are interchanged. The connection of this interpretation with the principle of equivalence has been discussed by Vigier.[25]

An attempt to overcome these difficulties has been given by several authors, in Refs. 27 and 28, and involves restricting the solutions of the Klein–Gordon equation to those that initially have time-like trajectories (as given by $\nabla_\mu S$) on the whole of space-time. It then folows, from the conservation of the current four-vector, that the particle motions remain time-like. While this result is correct it seems to be too severe a restriction, as it would involve a limitation on the relative amplitudes of two counter-propagating plane waves.[2,28] One could, at least in principle, use partially reflecting mirrors or barriers to adjust the amplitudes of the two beams to any desired ratio. The case of spin-one bosons is not essentially different in this respect, so one might consider using laser beams; there will then be regions where $\nabla_\mu S$ is a space-like four-vector. It would seem, therefore, that the use of the current four-vector, in the case of bosons, to define trajectories gives problems, whereas its use in the Dirac case[2,18] gives velocities less than c; this is due to the contribution from the spin current.

A problem that arises in both the fermion and boson case is that of the interpretation of the time component of the current vector as a probability density; this is thought to be problematic in the Klein–Gordon case, since j_0 need not be positive definite, whereas it is automatically so in the Dirac case. This problem can be overcome by linearizing the Klein–Gordon equation and separating the positive and negative energy solutions.[25,27,29] The interpretation of j_0, as a probability density, remains problematic, since it is the time-component of a four-vector. A theorem that has been used in this regard is that, if L_μ is a four-vector, with $\nabla_\mu L_\mu = 0$ and $L_\mu = 0$, except in a finite region of space, then $\int d^3x\, L_0$ is a constant Lorentz scalar. This theorem is, for example, invoked in classical electromagnetism, in showing that charge is conserved. It is, however, not applicable in the cases under consideration, since relativistic wavefunctions corresponding to positive (or negative) energies cannot be localized and, *a fortiori*, the current four-vector. If a covariant description is needed, one possibility that has been explored is the use of the evolution (or historical) time[30–32]; we are not aware, however, that the problem of superluminal velocities can be dealt with in this way.

A possible solution to the problems above is suggested by the fact that the construction of trajectories for the electron proceeds without the use of a Hamilton–Jacobi type equation; as remarked by J. Bell and Bohm, one only needs a guidance formula. Indeed, one may derive a Hamilton–Jacobi type equation for the electron, with a modified quantum potential, which leads to superluminal velocities, if one takes $\nabla_\mu S$ as the four-momenta. As we have seen, Bohm uses the Dirac equation in its noncovariant form and defines the three-velocity according to (18). This formulation is identical with de Broglie's, who also shows that with the neglect of spin, one obtains the Hamilton–Jacobi equation for the Klein–Gordon equation.[2] It has been known for some time that a linearized set of equations can be used to deal with bosons and fermions, and that they take the same form as the covariantly formulated Dirac equation. The Kemmer–Duffin–Petiau equation,[26] for example, is a five-component wave equation describing a spin-zero particle; the five components being a scalar function and its four derivatives. As Kemmer remarks, the content of these equations is the same as in de Broglie's theory in which he treats the photon as a fusion of two spin-one-half particles. If one selects a particular frame of reference, the equation takes the same form as the Dirac equation, and the velocity may be calculated in the same way. The result is related to the stress-energy-momentum tensor for this system and is easily shown to have a value less than c. In this theory, a spin operator appears whose expectation value is always zero, but which will contribute when calculating the current vector. In addition one either must assume that some natural frame of reference

occurs, relative to which the velocity may be calculated,[12] or one may find that the quantum field itself defines a unique time-like eigenvector of the stress-energy-momentum tensor. It is not clear that time-like eigenvectors always exist, although in one spatial dimension it may easily be shown that they do. Details of the above will appear in a subsequent publication.

It seems, therefore, that massive bosons may be treated as particles as de Broglie wanted, and will have subluminal velocities. The case of massless bosons will need separate consideration. We find that for massive bosons at least there is a choise of two causal theories, both of which can account for the predictions of the usual theory. In a further publication we compare, in detail, the application of these disparate approaches to the same set of model experiments, so as to elucidate the description of nature entailed in each case.

9. EXPERIMENTAL DISTINCTIONS BETWEEN THE DIFFERENT INTERPRETATIONS OF QUANTUM MECHANICS?

Among the followers of Bohm and de Broglie, there has been disagreement concerning the question of testability. Bohm and Hiley have argued that since the statistical predictions of their approach are identical to those of quantum mechanics, there can be no experimental test of the approach unless one adds further assumptions, e.g., the stochastic background or finite speed propagation of the quantum potential.

Vigier takes a different approach and has proposed a series of experiments which, it is claimed, allow such a distinction, given certain auxiliary assumptions (see Sect. 9.2). He claims that these experiments find a natural interpretation in the de Broglie–Bohm model, but not in the orthodox interpretations (of course the statistical predictions of quantum theory themselves are not in dispute).

Selleri and others have also proposed experiments designed to demonstrate the existence of quantum waves. Again, however, one must be very clear about the additional assumptions being made. In interpreting de Broglie, Selleri *et al.* claim that the real waves in physical space, which de Broglie referred to as the *u*-waves, each obey a single-particle, local wave equation. The consequence of this is, of course, that the approach advocated by Selleri contradicts the predictions of quantum mechanics.

[12] For example, one may have, to a good approximation, a Robertson–Walker metric and a definite time axis.

Under Selleri's assumption, there are no configuration-space waves and hence there is no possibility of nonlocal phenomena. It is then a problem, for approaches such as Selleri's, to explain the wealth of experimental data which confirms many-body quantum mechanics so well. Selleri *et al.* have therefore attempted to show that each experimental situation to date, which confirms many-particle quantum mechanics, can in fact also be accounted for by a local theory.

9.1. The Detection of the Broglie Waves

Franco Selleri was the first to suggest the experimental testability of the de Broglie waves, in 1969.[33] In the type of experiment proposed by Selleri, it is assumed that de Broglie waves in physical space carry neither energy nor momentum, but nevertheless, their existence can be demonstrated by the generation of zero-energy-transfer stimulated emission in a laser gain tube. This idea has been pursued by several other authors,[34] but so far no direct experiment to test this assumption has been performed. The Blake–Scarl experiment,[35] although controversial, has been interpreted as providing indirect evidence in favor of the reality of the de Broglie waves.

Prompted by the experiment performed by Pfleegor and Mandel,[36] several experiments have been proposed by Garuccio, Popper, and Vigier,[39] by Croca, Garuccio, Lepore, and Moreira,[41] and by Croca.[40] All these experiments are based on the notion that particles (even photons) follow well-defined trajectories, and that quantum waves evolve in physical space.

In the Pfleegor and Mandel experiment, two laser sources, locked in phase, produce an interference pattern even in those case in which only a single photon is in the superposition region at a time. The notion that photons are to be treated in just the same manner as material particles, from the de Broglie point of view, yields a conceptually simple explanation of the Pfleegor Mandel experiment. In this case each photon is a localized object in an extended wave, the form of which guides the particle-like object into the bright fringes. This seems a simple explanation, but it entails a program in which, as we have seen, there are the formidable mathematical difficulties, mainly associated with the definition of photon trajectories.

Furthermore, if one wishes to maintain that the waves associated with the photon are local, then one is faced with the task of accounting for the wealth of experimental evidence provided by quantum optical experiments,[36,37,43] which demonstrate nonlocal correlations. The Bohm theory for photons, as we have seen, is conceptually rather different; the Pfleegor Mandel experiment, for example, has a totally different explanation using this theory.[20]

Selleri and Schmidt[42] have proposed an experiment to test existence of local Selleri–de Broglie waves. It should be emphasized that the theory of these local waves is not developed and that what is proposed contradicts the statistical predictions of quantum theory. *It is an essentially different theory to quantum theory.* We do not enter into a discussion here, except to point out that an experimental test of the Selleri local guided-wave theory for photons has actually been performed by Wang, Zou, and Mandel,[43] following the proposal put forward in Ref. 41. The experimental outcome is compatible with the predictions of quantum field theory (and, we must emphasize, the Bohm interpretation) but in contradiction with the local Selleri model for photons, as was stated and applied in Ref. 41.

An attempt to salvage Selleri's local wave theory has been made in Ref. 44, where it was shown that, using only the idea of local waves in physical space and the assumption of a variable detection probability, it is possible to fit the experimental data of Ref. 43. In this account the photon detection probability is dependent on the quantum state and is thus not constant, as is in usual quantum field theory where, for a given state, the detection probability depends only on the "quantum efficiency" of the detectors. This notion has been the subject of much debate in the context of local explanation of EPR-type correlation experiments,[33,42,44] and we do not entertain this particular idea further in this paper. That quantum statistics can also be derived from a local model is the subject of another paper by one of us (MS) and Selleri.

9.2. The Experiment of Vigier *et al.*

In this section we discuss the proposed experiment of Vigier *et al.* The aim of this experiment is to demonstrate that quantum mechanical objects may display their wave and particle aspects at the same time, thereby contradicting the principle of complementarity. The experiment fails to invalidate complementarity, as it only provides indirect evidence of the coexistence of trajectories and interference; however, it certainly demonstrates that the de Broglie–Bohm picture of quantum objects, in terms of both particles and a waves, is one obvious and convincing description of these experiments.

The experiment is related to Young's double-slit interference experime, in which we observe the wave properties of quantum mechanical objects in the interference pattern formed from individual spots on the screen. These spots indicate the existence of particle-like properties in quantum objects; however, despite the presence of these spots, we are not able to specify

which slit any "particle" passed through on its way to the screen. If we devise some means of revealing, with increasing certainty, which slit a particle did pass through, for example, by measuring the transfer of momentum to the screen, then the visibility of the interference pattern is correspondingly diminished.[46] In the usual interpretation of quantum mechanics, we are led to believe that the only consistent way of thinking about this experiment is by denying the existence of a particle trajectory between source and screen altogether.

The aim of the proposed neutron interferometry experiments of Vigier *et al.*[4] was to attempt to detect the particle and wave aspects of neutrons simultaneously. The neutron was chosen because, unlike the photon, it is known to be massive with an internal structure, so that its particle properties are more evident than those of the photon.

A pulsed neutron beam, which is polarized vertically with respect to the apparatus, is incident upon a perfect crystal interferometer. There is, at any one time, at most one neutron inside the interferometer. The beam is split at the first set of crystal planes to produce two neutron beams, both in the spin-up state. A rotatable aluminum slab, in the path of both beams, provides a variable scalar phase-shift between the two beams.

These beams then both pass through radio-frequency (r.f.) spin-flip coils and are superposed beyond the final set of crystal planes, producing an interference in the measured intensity, which varies at one position in space with the value of the scalar phase shift. The neutrons which emerge from the interferometer, and whose detection is used to build up the interference pattern, each undergo time-of-flight measurements on the way to the detectors. Their energy is compared with that of unflipped neutrons to reveal whether or not the neutrons, which have passed through the coils, have the energy associated with the spin-down state, i.e., have actually been flipped.

If the energy of each neutron detected in the interference pattern is that associated with the spin-down state, then every neutron detected has undergone a spin-flip within the interferometer, and hence also an energy transfer $\hbar\omega_{rf}$. There are no resonant frequencies provided by the r.f. field which correspond to half the energy of a spin-flip, only to the full spin-flip energy. This means that if we assume that energy and momentum are conserved in each energy exchange, then each neutron must have lost a photon of energy in one coil or the other, not in both. Thus the results of this experiment may provide indirect evidence of the existence of neutron trajectories through the interferometer. It is also possible to obtain interference in the intensity of detected neutrons in the same experimental set-up. This implies that particle properties coexist with wave properties, for single neutrons. Possible trajectories for the neutron, at the last set of

crystal planes, are shown in Fig. 5 and 7, for different settings of the phase shifter.

To believe in the completeness of quantum mechanics is to deny the existence in this experiment of neutron trajectories, and to believe instead that absorption takes place in both r.f. coils, without the presence of energy conservation. It is certainly possible to maintain this point of view; however, since we have already shown, in Sec. 4.2 that Bohm's interpretation provides a consistent account of this experiment in terms of particle trajectories, the experiment highlights the fact that a much more intuitive approach to quantum mechanics may be provided than is generally, by the orthodox interpretation.

9.3. The Experiment of Ghose *et al.*

Ghose *et al.*[5] have proposed an experiment designed to show that both wave and particle characteristics may be displayed by light, at the same time, with the aim of demonstrating the inadequacy of the Copenhagen interpretation. In the proposed experiment, pulses of light in "single photon states" are incident upon two prisms as in Fig. 21. According to quantum optics, when the wavelength of the incident light is less than the separation of the two prism faces, the light will suffer total internal reflection within the first prism. In that event, all photon counts take place in a counter C_1, placed in the path of the reflected light. However, if the wavelength of incident light exceeds the interprism gap, quantum optics predicts that quantum tunneling of the light across the gap between the prisms occurs, and that the light may enter a photon counter C_2, placed beyond the second prism.

It is predicted that the two counters will click in perfect anticoincidence. The authors claim that such behavior strongly suggests that these packets of light are composed of single particles, which are either reflected at the first prism–air interface, or which enter the second prism by tunneling through the airgap. Since they consider the presence of tunneling to be accounted for by assigning a wave aspect to the photon, they suggest that the complementarity of the wave and particle aspects of quantum objects has been disproved, in this experiment.

However, just as in the original Young's two-slit interference experiment, the particle path is not directly observed—only the click in the detector; so the most that can be deduced from the results of this experiment is that the Copenhagen interpretation does not provide any causal explanation of the experiment and that a realist interpretation, in terms of particle trajectories, would be a useful and natural description of the

experiment, if it were possible to provide one. As we have seen, there is not as yet a complete causal theory for light, in terms of photon particle trajectories; but it would be reasonable to assume that the form of the trajectories, if they exist, are similar to those of other quantum objects, such as neutrons, since it is possible to reproduce some of the interference phenomena of light using the wave equation for massive particles.[47]

We might conjecture that the form of the trajectories for photon tunneling through the barrier between the prisms, in the Ghose experiment, is similar to those calculated nonrelativistically for a massive particle, as is done in Sec. 4. Alternatively, we can provide a deterministic model for the behavior of the light in terms of a quantum field theory, where the hidden variable representing the field is not the photon position, but the coordinates of the field modes, as was discussed in Sec. 7.1.

REFERENCES

1. L. de Broglie, *C. R. Acad. Sci. (Paris)* **183**, 447 (1926); **185**, 580 (1927).
2. L. de Broglie, *Nonlinear Wave Mechanics* (Elsevier, Amsterdam, 1960).
3. D. Bohm, *Phys. Rev.* **85**, 166, 180 (1952).
4. N. Cufaro-Petroni and J. P. Vigier, *Found. Phys.* **22**, 1 (1992).
5. P. Ghose, D. Home, and G. S. Agarwal, *Phys. Lett. A* **158**, 8–9 (1991).
6. B. D'Espagnat, *Conceptual Foundations of Quantum Mechanics* (Benjamin, California, 1971).
7. M. Jammer, *The Philosophy of Quantum Mechanics* (Wiley, New York, 1974).
8. J. S. Bell, *Found. Phys.* **12**, 989 (1982).
9. C. Dewdney and B. J. Hiley, *Found. Phys.* **12**, 27 (1982).
10. C. Dewdney, *Phys. Lett. A* **109**, 377 (1985).
11. C. Dewdney, P. R. Holland, and A. Kyprianidis, *Phys. Lett. A* **119**, 259 (1986).
12. C. Dewdney, P. R. Holland, and A. Kyprianidis, *J. Phys. A* **20**, 4717 (1987).
13. D. Bohm, R. Schiller, and J. Tiomno, *Suppl. Nuovo Cimento* **1**, **48** (1955).
14. C. Dewdney and M. M. Lam, "What happens in a quantum transition?" in *Information Dynamics*, H. Atmanspacher and H. Scheingraber, eds., NATO ASI Series B, Physics Vol. 256 (Plenum Press, New York, 1990).
15. C. Dewdney, A. Kyprianidis, and J. P. Vigier, *J. Phys. A* **17**, L741 (1984).
16. C. Dewdney and P. R. Holland, in *Quantum Implications*, B. J. Hiley and F. D. Peat, eds. (Methuen, New York, 1987).
17. C. Dewdney, "Constraints on quantum hidden variables and the Bohm theory," *J. Phys. A* **25**, 3615 (1992).
18. D. Bohm, *Prog. Theor. Phys.* **9**, 273–287 (1953).
19. D. Bohm and B. J. Hiley, *The Undivided Universe*, unpublished manuscript of forthcoming book.
20. D. Bohm, B. J. Hiley, and P. Kaloyerou, *Phys. Rep.* **144**, 6, 349–375 (1987).
21. M. M. Lam and C. Dewdney, "Cavity quantum scalar field dynamics: the Bohm approach. Part I: the free field; Part II: the interaction of the field with matter," to be published.
22. J. L. Synge, *Relativity: The Special Theory* (North-Holland, Amsterdam, 1965).

23. R. Penrose and W. Rindler, *Spinors and Space-Time*, Vol. 2 (Cambridge University Press, Cambridge, 1986).
24. C. Fenech and J. P. Vigier, *C. R. Acad. Sci. (Paris)* **293**, 249 (1981).
25. P. R. Holland and J. P. Vigier, *Nuovo Cimento* **88B**, 20 (1985).
26. N. Kemmer, *Proc. Roy. Soc. A* **173**, 91 (1939).
27. N. Cufaro-Petroni, A. Kyprianidis, Z. Maris, D. Sardelis, and J. P. Vigier, *Phys. Lett. A* **101**, 4 (1984).
28. A. Kyprianidis, *Phys. Lett. A* **111**, 111 (1985).
29. H. Feshbach and V. Villars, *Rev. Mod. Phys.* **30**, 24 (1958).
30. P. Kaloyerou and J. P. Vigier, *J. Phys. A, Math. Gen.* **22**, 663 (1989).
31. J. R. Fanchi and W. J. Wilson, *Found. Phys.* **13**, 6, 571 (1983).
32. E. C. G. Stuckelberg, *Helv. Phys. Acta* **14**, 372, 588 (1941); **15**, 23 (1942).
33. F. Selleri, *Nuovo Cimento Lett.* **1**, 908 (1969); *Found. Phys.* **12**, 1087 (1982).
34. J. and M. Andrade e Silva, *C. R. Acad. Sci. (Paris)* **290**, 501 (1980); A. Garuccio, V. Rapisarda, and J. P. Vigier, *Phys. Lett. A* **90**, 17 (1982); R. Giovanelli, "Detection of empty waves by means of photon correlations in amplified light pulses," in *Microphysical Reality and Quantum Formalism*, A. van der Merwe, F. Selleri, and G. Tarozzi, eds. (Reidel, Dordrecht, 1985).
35. G. D. Blake and D. Scarl, *Phys. Rev. A* **19**, 1948 (1979).
36. R. L. Pfleegor and L. Mandel, *Phys. Rev.* **159**, 1084 (1967); *J. Opt. Soc. Am.* **58**, 946 (1968).
37. L. Mandel, *Am. Phys. Soc.* **28**, 929–943 (1983); R. Ghosh, C. K. Kong, and L. Mandel, *Phys. Rev. A* **34**, 5 (1986); R. Ghosh and L. Mandel, *Phys. Rev. Lett.* **59**, 17 (1987); Z. Y. Ou and L. Mandel **61**, 1 (198).
38. L. de Broglie and J. Andrade e Silva, *Phys. Rev.* **172**, 1284 (1968).
39. A. Garuccio, K. R. Popper, and J. P. Vigier, *Phys. Lett. A* **86**, 8, 397 (1981).
40. J. R. Croca, *Found. Phys.* **17**, 971 (1987).
41. J. R. Croca, A. Garuccio, and V. L. Lepore, *Found. Phys. Lett.* **3**, 557 (1990).
42. M. Schmidt and F. Selleri, *Found. Phys. Lett.* **4**, 1 (1991).
43. L. J. Wang, X. Y. Zou, and L. Mandel, *Phys. Rev. Lett.* **66**, 1111 (1991).
44. F. Selleri, "Two-photon interference and the question of empty waves," in *Bell's Theorem and the Foundations of Modern Physics*, A. van der Merwe, F. Selleri, and G. Tarozzi, eds. (World Scientific, Singapore, 1992).
45. J. S. Bell, *Rev. Mod. Phys.* **38**, 4747 (1966).
46. W. Wooters and W. H. Zurek, *Phys. Rev. D* **19**, 473–484 (1979).
47. M. M. Lam and C. Dewdney, *Phys. Lett. A* **150**, 34 (1990).
48. D. Bohm and J. P. Vigier, *Phys. Rev.* **96**, 208–216 (1954).